Manuscript Details

Manuscript number PRECAM_2018_114_R1

Title Petrology, physical volcanology and geochemistry of a Paleoproterozoic large igneous province: The Hekpoort Formation in the southern Transvaal sub-basin (Kaapvaal Craton).

Article type Research Paper

Abstract

The ~ 2.23 Ga Hekpoort Formation (Transvaal sub-basin) and the ~ 2.43 Ga Ongeluk Formation (Griqualand West sub-basin) represent voluminous Paleoproterozoic igneous events on the Kaapvaal craton of South Africa that predate the emplacement of the ~ 2.055 Ga Bushveld Complex, and probably covered most of the craton at the time of their extrusion. In this contribution, we present a field, petrological and geochemical study of the Hekpoort Formation and compare it with the Ongeluk Formation. The Hekpoort Formation consists of a thick subaerial volcanic sequence in which volcanoclastic rocks occur mainly at the base. Rare, localized hyaloclastites and variolitic rocks record the presence of ponded water, while interbedded sedimentary rocks and paleo-weathered flow tops suggest prolonged time-breaks in volcanic activity. The Hekpoort rocks underwent metamorphism up to greenschist facies but also episodes of metasomatism and silicification. Preserved primary magmatic minerals are clinopyroxene (pigeonite, augite and diopside), and rarely plagioclase (labradorite). Both the variable whole rock Mg# (evolving from 69 to 50) and the change in clinopyroxene composition attest to magmatic fractionation. Lava units of both the Hekpoort and Ongeluk formations are mostly basalts, with silicification responsible for increased SiO2 contents. Lava units of both formations also display remarkably similar trace elements patterns, which is noteworthy for units separated by 200 million years, and unique among the Precambrian mafic magmatic units of the Kaapvaal craton that we evaluated. Similar to other Precambrian mafic magmatic units of the Kaapvaal craton, the Hekpoort Formation shows an arc-like trace element signature, mainly represented by negative Nb-Ta anomalies (in normalized trace element patterns). The Hekpoort (and Ongeluk), together with three other Paleoproterozoic mafic units of the craton older than 2.2 Ga, exhibit relatively high contents of Th and U, which sharply contrasts with Archean units. The data suggest that a subduction process marked the Archean-Proterozoic boundary on the Kaapvaal craton.

Keywords Hekpoort and Ongeluk formations; Kaapvaal craton; Paleoproterozoic within-craton volcanism; Archean-Proterozoic boundary; Large Igneous Province; Geochemistry.

Corresponding Author Fabien Humbert

Corresponding Author's Institution University of Johannesburg

Order of Authors Fabien Humbert, Michiel de Kock, Wladyslaw Altermann, Marlina Elburg, Nils Lenhardt, Albertus Smith, Samson Masango

Suggested reviewers Julian Pearce, Janet Hergt, Karen Fontijn, Richard Ernst, Grant Cawthorn

Petrology, physical volcanology and geochemistry of a Paleoproterozoic large igneous province: The Hekpoort Formation in the southern Transvaal sub-basin (Kaapvaal Craton).

Fabien Humbert [a], Michiel O. de Kock[a], Wladyslaw Altermann[b], Marlina A. Elburg[a], Nils Lenhardt[b], Albertus J. B. Smith[a], Samson Masango[b]

[a] Department of Geology, University of Johannesburg, PO Box 524, Auckland Park 2006, Johannesburg, South Africa

[b] Department of Geology, University of Pretoria, Pretoria 0002, South Africa

Accepted *date*. Received *date*; in original form *date*

Abbreviated title: Paleoproterozoic Hekpoort LIP, RSA

* Corresponding author:

Email: humbert.fabien@gmail.com

Phone: +27 (0)76 258 1760

Fax: +27 (0)11 559 4702

Abstract

The ~ 2.23 Ga Hekpoort Formation (Transvaal sub-basin) and the ~ 2.43 Ga Ongeluk Formation (Griqualand West sub-basin) represent voluminous Paleoproterozoic igneous events on the Kaapvaal craton of South Africa that predate the emplacement of the ~ 2.055 Ga Bushveld Complex, and probably covered most of the craton at the time of their extrusion. In this contribution, we present a field, petrological and geochemical study of the Hekpoort

Formation and compare it with the Ongeluk Formation. The Hekpoort Formation consists of a thick subaerial volcanic sequence in which volcanoclastic rocks occur mainly at the base. Rare, localized hyaloclastites and variolitic rocks record the presence of ponded water, while interbedded sedimentary rocks and paleo-weathered flow tops suggest prolonged time-breaks in volcanic activity. The Hekpoort rocks underwent metamorphism up to greenschist facies but also episodes of metasomatism and silicification. Preserved primary magmatic minerals are clinopyroxene (pigeonite, augite and diopside), and rarely plagioclase (labradorite). Both the variable whole rock Mg# (evolving from 69 to 50) and the change in clinopyroxene composition attest to magmatic fractionation. Lava units of both the Hekpoort and Ongeluk formations are mostly basalts, with silicification responsible for increased SiO_2 contents. Lava units of both formations also display remarkably similar trace elements patterns, which is noteworthy for units separated by 200 million years, and unique among the Precambrian mafic magmatic units of the Kaapvaal craton that we evaluated.

Similar to other Precambrian mafic magmatic units of the Kaapvaal craton, the Hekpoort Formation shows an arc-like trace element signature, mainly represented by negative Nb-Ta anomalies (in normalized trace element patterns). The Hekpoort (and Ongeluk), together with three other Paleoproterozoic mafic units of the craton older than 2.2 Ga, exhibit relatively high contents of Th and U, which sharply contrasts with Archean units. The data suggest that a subduction process marked the Archean-Proterozoic boundary on the Kaapvaal craton.

Key words: Hekpoort and Ongeluk formations; Kaapvaal craton; Paleoproterozoic within-craton volcanism; Archean-Proterozoic boundary; Large Igneous Province; Geochemistry.

1. Introduction

The Neoarchean to Paleoproterozoic (~ 2.65 – 2.06 Ga) Transvaal Supergroup of the Kaapvaal craton (Fig. 1) is described from three sub-basins (i.e., the Griqualand West, Kanye and Transvaal sub-basins). The successions preserved in these sub-basins are similar, with correlation being the best for the lower chemical sedimentary units, and the poorest for the upper sedimentary and volcanic lithologies (e.g., *Eriksson et al., 2006*). These upper lithologies are represented by the Postmasburg Group in the Griqualand West sub-basin, and the Pretoria Group within the Transvaal sub-basin (Fig. 2). The Hekpoort Formation (Pretoria Group) is the best developed of the volcanic events in the Transvaal sub-basin, and is mainly composed of basaltic lava flows with minor lenses of volcanoclastic rocks. Based on its areal extent of ca. 100,000 km^2 and maximum thickness of up to 1100 m (e.g., *Lenhardt et al., 2012*), the Hekpoort Formation can be classified as a large igneous province (LIP) (*Ernst, 2014*).

In the Griqualand West sub-basin, the Ongeluk Formation (e.g., *Grobler and Botha, 1976*; *Cornell et al., 1996; Gutzmer et al., 2003*) is a volcanic unit of comparable thickness. The two volcanic formations were long correlated based on lithostratigraphy (e.g., *du Toit, 1929*; *Moore et al., 2001*; *Eriksson et al., 2006*; *Lenhardt et al., 2012*). Similar isotopic dates determined from the Hekpoort Formation, 2224 ± 21 Ma (*Burger and Coertze, 1973*; whole rock Rb-Sr isochron), and 2222 ± 13 Ma for the Ongeluk Formation (*Cornell et al., 1996*; whole rock Pb–Pb isochron) supported this longstanding correlation. This temporal equivalence was the basis for correlations between the Pretoria and the Postmasburg groups from the Transvaal to the Griqualand West sub-basins, across the Kaapvaal craton. Apart from these volcanic units, the groups represent dissimilar sedimentary units and differing unconformity-bound sequences (*Eriksson et al., 1995; 2006*) (Fig. 2). Radiometric data are scarce in the two groups and sometimes contradictory; e.g., the 2222 ± 13 Ma of the Ongeluk Formation does not agree with the ca. 2.4 Ga Pb-Pb and U-Pb whole rock carbonate ages for the overlying Mooidraai Formation (Fig. 2).

Recently, workers have questioned the temporal equivalence of the two volcanic formations, based on stratigraphic arguments (*Moore et al., 2001*; *Hoffman, 2013*), carbonate Pb-Pb and U-Pb geochronological results (*Bau et al., 1999*; *Fairey et al., 2013*), and detrital zircon U-Pb age data (*Moore et al., 2012*). *Gumsley et al. (2017)* reported the age of the Ongeluk Formation to be 2426 ± 3 Ma based on baddeleyite dating, while *Humbert et al. (2017)* showed that the paleomagnetic poles for the Ongeluk and Hekpoort formations differ from each other (the Ongeluk paleopole being characterized by *Evans et al., 1997*). Additionally, the correlation between the Pretoria and Postmasburg groups is unconvincing (Fig. 2). Nevertheless, several conspicuous similarities, such as geochemistry, exist between the two formations (*Cornell et al., 1996*; *Oberholzer and Eriksson, 2000*).

In this work, we present a volcanological, petrological and geochemical study of the Hekpoort Formation from the southern part of the Transvaal sub-basin (Fig. 1). Despite the recently highlighted age difference between the Hekpoort and Ongeluk formations (*Gumsley et al., 2017*), we compare the geochemical data for the two formations. The now apparent ca. 200 myr difference in age makes this comparison significant for the discussion of the regional correlation between the two formations and their possible equivalents on the Pilbara Craton in Western Australia (*Cheney et al., 1996*; *Nelson et al., 1999*; *Van Kranendonk et al., 2012*). Additionally, it has bearing on important events in earth history like the Great Oxidation Event and the paleosols of these formations (e.g., *Holland and Beukes, 1990*; *Wiggering and Beukes, 1990*; *Ohmoto, 1996*; *2004)*, as well as on the possible appearance of early eukaryotes in the Paleoproterozoic *(Retallack et al., 2013*; *Bengtson et al., 2017*), and the timing and the regional extent of the Paleoproterozoic glaciation and the snowball earth theory (*Evans et al., 1997*; *Hoffman et al., 1998*; *2013*; *Eriksson and Altermann, 2013*).

2. Geological setting and description of the studied area

2.1. The Pretoria Group and Hekpoort Formation

The lowermost Pretoria Group is represented by the Duitschland, Rooihoogte and Timeball Hill formations (Fig. 2), and rests with a marked unconformity on the Chuniespoort Group carbonates and banded iron formation successions below (*Eriksson et al., 2006*; *Schröder et al., 2016*). The Timeball Hill Formation is overlain by the Boshoek Formation conglomerate. The fluvio-glacial origin of this conglomerate, despite the lack of evidence for the glacial facies, has been hitherto defended because of the assumed age equivalence to the Ongeluk Formation, which rests on the clearly glacial Magkanyene Formation in Griqualand West (Fig. 2). The Hekpoort Formation rests conformably on the Boshoek Formation (*Eriksson et al., 2006*; *Eriksson and Altermann, 2013*). The upper part of the Hekpoort Formation is in most places erosionally removed by the unconformity at the base of the fluvial Dwaalheuwel Formation quartzite (Figs. 3a and 4d). This unconformity is marked in places by the Hekpoort oxic paleosol that has been used to date the Great Oxidation Event (*Button, 1986*; *Holland and Beukes, 1990*; *Eriksson and Cheney, 1992*; *Yang and Holland, 2003*; *Retallack, 2013*), and by the possible early appearance of the first terrestrial eukaryotes (*Retallack et al., 2013*; *Bengtson et al., 2017*). Quartzites and shales of the Strubenkop Formation overlie the continental sandstones and conglomerates of the Dwaalheuwel Formation (*Eriksson et al., 2006*).

Rocks in the Transvaal sub-basin have undergone only very slight deformation before two major events around 2.0 Ga. In the north central part of the Transvaal sub-basin, the Pretoria Group was intruded by 2054.89 ± 0.37 Ma (*Zeh et al., 2015*) magmas of the Bushveld Complex (Figs. 1 and 2), the world's largest known layered mafic intrusion (~0.5 – 1×10^6 km^3; e.g., *Letts et al., 2009*), causing regional low-grade and contact metamorphism (*Eriksson et al., 1995*; *2006*). The Bushveld Complex is but a part of a much larger regional LIP (the Bushveld LIP) which includes the Molopo Farms layered intrusion, the Okwa basement complex, and smaller intrusive bodies of the Bushveld high-Ti suite near the Vredefort impact structure and associated carbonatites (Schiel and Phalborwa) (e.g. *Rajesh et al., 2013*; *Ernst, 2014*).

In the south-western part of the sub-basin, the Pretoria and underlying Chuniespoort groups have been affected by the 2023 ± 4 Ma Vredefort impact structure (VIS; *Kamo et al., 1996*) representing the vestiges of an immense (250–300 km original diameter) impact crater (*Henkel and Reimold, 1998*) (Fig. 1). *Humbert et al. (2017),* have documented the effects of the Bushveld LIP and the VIS on most of the Hekpoort rocks in the southern Transvaal sub-basin.

The 50–1110 m thick volcanic Hekpoort Formation is characterized by intercalated lava flows, pyroclastic deposits, and their reworked counterparts (*Oberholzer, 1995*), representing deposition in a subaerial environment (e.g*., Button, 1973*; *1986; Eriksson and Reczko, 1995*; *Oberholzer, 1995*). The Hekpoort Formation sharply overlies either the mudrocks of the Timeball Hill Formation (Figs. 3a and 4a, b), or the Boshoek Formation conglomerates and sandstones (Figs. 2 and 3; *Cheney, 1996*).

Several overlapping radiometric ages have been determined for the Hekpoort Formation. Dates of 2236 ± 38 Ma (whole rock Pb–Pb isochron; *Cornell et al., 1996*) and 2224 ± 21 Ma (whole-rock Rb–Sr isochron; *Burger and Coertze, 1973*) represent direct dating of the lavas. U-Pb SHRIMP dating of detrital zircons from palaeosols or interbedded sedimentary units in the formation yielded a maximum age of 2247 ± 10 Ma (*Schroeder et al., 2016*).

2.2. The Ongeluk Formation of the Postmasburg Group

In the Griqualand West sub-basin, the Ongeluk Formation (Fig. 1), which belongs to the Postmasburg Group (Fig. 2), is characterized by an up to 900 m-thick succession of massive basalts, pillow lavas and hyaloclastites indicating terrestrial and subaqueous extrusion of the volcanic rocks along the submerged western margin of the Kaapvaal craton (e.g*., Cornell et al.,* *1996*). The Ongeluk Formation unconformably to disconformably overlies the Makganyene Formation glaciogenic deposits (*Altermann and Hälbich, 1991*); locally, however, it is also conformable, probably in deeper lacustrine facies (*Moore et al., 2001*; *Altermann et al., submitted*). In the northern parts of the sub-basin it is overlain by manganiferous banded iron formations and dolostones that constitute the Hotazel and Mooidraai formations (Fig. 2).

In the northern part of the Griqualand sub-basin the sequence above the Ongeluk Formation does not contain any unconformities or disconformities. The Hotazel Formation (Mn-BIF deposits) follows on the lavas and is overlain by the Mooidraai Formation (dolomites). Contrary to older, Rb/Sr whole rock age data for the Ongeluk Formation, clustering around 2222 ± 12 Ma (*Cornell et al., 1996*), *Bau et al. (1999)* and *Fairey et al. (2013)* dated the Mooidraai Formation respectively at 2394 ± 26 Ma (whole rock Pb-Pb isochron) and 2392 ± 23 Ma (whole rock U-Pb isochron). This apparent contradiction has now been resolved by dating of baddeleyite from a sill intruding the Ongeluk Formation at 2426 ± 3 Ma (*Gumsley et al., 2017*). This date further sets a maximum age for the lower Proterozoic snow ball earth glaciation, represented by the underlying Makganyene Formation, being clearly older than the previously tentatively correlated Boshoek conglomerate in the Transvaal sub-basin. However, the intriguing similarities between the Ongeluk and Hekpoort formations remain, and are not only geochemical (see below) but also pertain to stratigraphy and depositional facies. Both formations start mainly as terrestrial outflows unconformably covering coarse-grained (conglomeratic) terrestrial deposits and both contain oxic paleosols that have served as evidence in the discussion of the timing of the Great Oxidation Event (*Wiggering and Beukes, 1990; Shibuya et al., 2017*; *Retallack, 2013*) - which can now hardly be dubbed an “event” if it apparently lasted over 200 myr. The Ongeluk Formation is overlain by shelf deposits of the Hotazel Member manganiferous iron formation in the northern Griqualand West sub-basin whereas the Hekpoort Formation displays signs of subaquatic deposition, at least locally, in its upper part (*Button, 1974*). Moreover, microfossil evidence for early Proterozoic eukaryotes was found in the paleosols of both the Ongeluk (*Bengtson et al., 2017*) and the Hekpoort Formation (*Retallack et al., 2013*). Note that evidence for eukaryotic microfossils has been however discusses in the Kaapvaal craton for much older rocks, 2.74 Ga Ventersdorp Supergroup lacustrine carbonates (Kaźmierczak et al., 2016). Nonetheless, the timing of development of these paleosols can also be questioned; they could represent oxidative weathering at a much later stage and then not be paleosols.

2.4. General description of the studied areas

The Hekpoort Formation was studied in several places (Fig. 1): to the southwest of Johannesburg around the Vredefort impact structure (VIS), and northeast of Johannesburg. The formation has not been described in detail from these areas; only *Coetzee (2001*) worked on some Hekpoort Formation samples from boreholes drilled near Potchefstroom (i.e., boreholes DPZ2; RHK1). *Oberholzer and Eriksson (2000)* already studied the Hekpoort Formation in its type locality around the town of Hekpoort. We also did some field studies in this area, but did not sample, northwest of Johannesburg.

2.4.1. SW of Johannesburg (Potchefstroom syncline and Fochville monocline)

The Hekpoort Formation outcrops form two arcs that are wrapped around the VIS (Fig. 1). Outcrops are generally poor (Fig. 4c), but complete sections can be found in the Potchefstroom syncline (Fig. 4a, b) and in the monocline around Fochville (Fig. 1).

The Potchefstroom syncline (Fig. 1) is an asymmetrical fold on regional scale, with the major fold axis striking approximately NNE and a dip of bedding at 10-20° in easterly directions along its western limb and steeper dips of 30-35° towards westerly directions along the eastern limb. Folding postdates the extrusion of the Hekpoort lavas, and is possibly related to the VIS

(Fig. 4a), although an earlier E-W compression phase is probable, as the fold does not follow the general bedding trends paralleling the VIS rim. In this syncline the Hekpoort Formation directly overlies the Timeball Hill Formation (Fig. 3a) and is disconformably covered by sedimentary rocks of the Dwaalheuwel and Strubenkop formations, as witnessed in an outlier in the central part of the syncline (Fig. 4b). The Hekpoort Formation has a calculated maximum thickness of ca. 340 m (calculated from the measured apparent thicknesses and local dip angles), not taking erosion prior to deposition of Dwaalheuwel sedimentary rocks into account.

In the Fochville monocline (Fig. 1) the Hekpoort Formation also lies directly above the Timeball Hill Formation shales and is overlain by the siltstones of either the Dwaalheuwel or Strubenkop formations (Fig. 3a). A complete succession of the Hekpoort Formation crops out south of Wedela (Fig. 1); the outcrops become less complete eastward. The lavas at the top of the Hekpoort Formation present clear evidence of paleo-weathering marked by neocrystallisation of iron-rich phases (Fig. 4d; 'fresh' Hekpoort lavas are shown in Fig. 4e), attesting that the top contact corresponds to an unconformity. Both the sedimentary and igneous rocks are dipping gently (15-26°) to the SSE. The thickness of the Hekpoort Formation in this area is ca. 800 m, in agreement with estimates from the west of the Transvaal sub-basin, but thinner than the supposed 1100 m in the south (see *Lenhardt et al., 2012* for a review).

2.4.2. NE of Johannesburg (Mooikloof monocline)

In this area, the rocks of the Pretoria Group dip to the NE, below the Rustenburg Layered Suite of the Bushveld Complex. Here, the Hekpoort Formation is ca. 500 m thick (in agreement with northward thinning described by *Button, 1973*), with consistent northeasterly directed dip angles of 10-15°. However, small synclinal and anticlinal structures trending approximately E-W can be found. The Hekpoort Formation is locally developed on top of the Boshoek Formation conglomerate. The lowermost Hekpoort layers consist of hyaloclastites, and massive and amygdaloidal lavas, which are intercalated with thinly laminated siltstones and cherts (silicified laminated mudstones). Outcrops east of Mooikloof present the complete preserved succession of the Hekpoort Formation, which is overlain by the Strubenkop Formation in this monocline.

2.4.3. NW of Johannesburg (Hekpoort river valley)

This area contains excellent outcrops of extensive debris flow deposits, sedimented in an extensional setting which may constitute a graben (Fig. 3b). This graben may have stretched in an approximate E-W direction, thus perpendicular to younger graben structures in the region (e.g., the Hartbeespoort or Brits graben, cutting through younger stratigraphy). Conclusive with the interpretation of a graben is the significantly increased thickness of the Hekpoort Formation in this area. We measured it to be close to 1000 m, confirming the 1100 m estimated thickness by Lenhardt et al. (2012).

3. Field observations

3.1. General features

The Hekpoort Formation is composed mainly of thick successive lava flows interpreted as originating from a single magma pulse (i.e., similar to 'tabular-classic flows', *Jerram et al., 2000*). The lava flows have thicknesses of between 8 m and 60 m, and are often characterized by amygdaloidal flow tops with thicknesses between 0.5 to 1 m. These display an abundance of amygdales that are commonly coalesced, with anastomosing geometries (Fig. 4f). Amygdales are partially or completely filled with secondary minerals: mostly quartz, but also clinochlore, zeolite and calcite. The flow tops can be highly altered. *Coetzee (2001)* and *Lenhardt et al. (2012*) interpreted the alteration to be pervasive, but it could also represent periods of weathering between successive flows, as alteration seems to be restricted to flow tops. These apparent weathering horizons are more common near the base of the formation, which may suggest a lower initial eruption rate. However, all outcrops have a reddish hydroxide coating due to weathering (Fig. 4c, f, g).

The "*locally developed several meters-thick flow top breccias*" described by *Oberholzer and Eriksson (2000)* and *Coetzee (2001)* were encountered mainly close to the type locality. Additionally, in a few places we observed volcanoclastic materials (Fig. 4g), as mentioned in other studies (e.g., *Button, 1973*; *Sharpe et al., 1983*; *Oberholzer, 1995*; *Oberholzer and Eriksson, 2000*; *Coetzee, 2001*). While *Oberholzer and Eriksson (2000)* estimated that volcanoclastic rocks and lava flows occur in equal proportions, we only observed this in the Hekpoort area. In the other studied areas, our observations are more in agreement with *Button (1973)* and *Sharpe et al. (1983)* who suggested that lava flows predominate and that volcanoclastic rocks are concentrated towards the base of the Hekpoort Formation. *Button (1973)* estimated the quantity of volcanoclastic rocks as 10% in the east of the preserved Transvaal sub-basin. In the area we have studied, volcanoclastic rocks represent as little as 1% of outcrops and are only a minor occurrence.

3.2. Specific and local features

3.2.1. Features of massive lava flows

Shear induced outgassing or 'second order' lava flows

In section 3.1. we have described tabular-classic lava flows originating from a single magma pulse and locally (Table 1) showing evidence of palaeo-weathering before the emplacement of the next lava flow. Within such flows one can occasionally find laterally consistent layers (from 10 cm to 1 m in thickness) that are devoid of amygdales but separated by 1-4cm thick amygdale-rich layers (Fig. 5a, b). Such features could represent subordinate 'second order' lava flows; or they may be related to shear-induced outgassing (e.g., *Shields et* *al., 2016*), i.e., they are the result of differential internal flow during the spreading of a lava lobe due to heterogeneities in lava rheology (vesicularity, water content, microlite content, viscosity). Stretched morphologies of amygdales paralleling the flow direction were rarely observed (Fig. 5b). Such 'second order' lava flows could potentially be tabular-classic lava flows with a reduced thickness, either because of paleo-topographic reasons or because they correspond to the edge of a flow.

Vesicle cylinders

Amygdale concentrations in the form of oblique columns, cylinders or pipes are a fairly common feature in the Hekpoort lavas (Fig. 5b-f; Table 1). Such vesicle cylinders often display increasing diameters towards the top of flows; they formed after the host lava ceased all movement (*Santos Barreto et al., 2014*) and before the lava reached the temperature of glass transition. During cooling of the lavas, bubbles continue to grow, forming cylinders perpendicular to the solidification front (*Philpotts and Lewis, 1987*; *Godinot, 1988*; *McPhie et al., 1993*). Such cylinders highlight that the magma contained volatiles, although no more than 0.01 wt% H_2O is necessary for their formation (*Philpotts and Lewis, 1987*).

Vesicle cylinders are common features in mafic lavas (e.g., *Wilmoth and Walker 1993*; *Santos Barreto et al., 2014*), but some examples in the Hekpoort Formation are exceptional in size: the lengths of the vesicle cylinders can be 1-3 m (Fig. 5c), with a diameter from a few centimeters up to 30 cm. Smaller vesicle cylinders (e.g., Fig. 5b) are encountered throughout the Hekpoort Formation. The meter-scale large cylinders (Fig. 5c-f) were only observed at two locations (in the northern part of the Potchefstroom syncline and in the Mooikloof area). In each case, they were restricted to and concentrated within one or several 'second order' lava flows at the bottom of a single lava flow. The large vesicle cylinders occur in lavas otherwise macroscopically devoid of amygdales (Fig. 5d, g). Petrographic study of the large vesicle cylinders reveals an abundance of vesicles with various diameters (but less than 500 μm) homogenously distributed throughout these flows. This indicates that the flows that contain vesicle cylinders were richer in volatiles than other Hekpoort lavas; vesicle cylinders are formed by the exsolution of a gas phase from the crystallizing lava (*Philpotts and Lewis, 1987*; *Godinot, 1988*). The difference in color (Fig. 5g) between the host rock (darker) and the cylinder (lighter) is related to a difference in texture rather than a compositional difference. The cylinders are rich plagioclase and euhedral clinopyroxene and appear to be more crystalized than the lava around. The presence of chlorite in between these two minerals yet suggest that the lava was yet not primarily exactly holocrystalline. The host lava shows a hypocrystalline texture with euhedral clinopyroxene (similar in size than in the cylinders). The secondary minerals filling the amygdales are mainly quartz but also zeolites and clinochlore.

Not all of the vesicle cylinders are perfectly cylindrical (Fig. 5e, f); three types of cylinders can be discerned. The most common type consists of networks of cylindrical columns perpendicular to the flow surface with individual cylinder diameters ranging between 10 to 30 cm (Fig. 5c); these cylinders often widen upwards and show a relatively homogeneous distribution of amygdales (Fig. 5d). The second, relatively uncommon, cylinder type shows a higher concentration of amygdales close to one side of the cylinder (e.g., left side in Fig. 5e); the opposite side displays irregularly shaped amygdale concentrations, forming a net-like structure in a planar section. It is likely that the amygdale-rich areas correspond to the principal conduit of gas extrusion inside the cylinder before total solidification of the lava; at the same time, this conduit spread some gas laterally resulting in the ‘net of ridges’. The last type of vesicle cylinder shows ellipsoid shapes in planar sections paralleling what seems to be the flow direction (Fig. 5f). They might correspond to the tops of type-one cylinders (C-S cylinder sheets of *Santos Barreto et al., 2014*), where different solidification fronts advanced in the lava flow when it was still in motion. Yet, the amygdales are mainly homogeneously distributed within one cylinder and do not present evidence of flow. Unfortunately, no outcrop allowed for a direct comparison between the three types.

Pahoehoe lava

Pahoehoe or ropy lava can be found locally (Fig. 5h; Table 1); until now such features have not been described from the Hekpoort Formation. As only two occurrences of pahoehoe lava outcrops were found (in the area around Fochville), these were not sampled in order to preserve the outcrops. Field observations show few amygdales within these pahoehoe flows, and they are thus likely to be massive, rather than the spongy (S-type) pahoehoe (*Wilmoth and Walker, 1993*).

3.2.2. Volcanoclastic rocks

As emphasized in the section 3.1, outcrops of volcanoclastic rocks are typically small, making it difficult to determine their pyroclastic or epiclastic nature. Nevertheless, the observations below highlight that some of them have experienced minimal or no sedimentary reworking. Three types of volcanoclastic rocks were identified: stratified lapilli-tuff, massive lapilli- / tuff-breccia, and pyroclastic breccia. The more extensive deposits in the Hekpoort river valley are discussed separately at the end of this section.

Stratified lapilli-tuff

Previous studies (e.g., *Oberholzer, 1995*; *Oberholzer and Eriksson, 2000*; *Lenhardt et al., 2012*) described thick (ca. 60 m) lapilli-tuffs near the town of Hekpoort (*Oberholzer and Eriksson, 2000*). In other areas, we only found minor amounts of lapilli-tuff, locally in the lowest part of the Hekpoort Formation: boulders of tuffaceous material were seen in the far western part of Johannesburg, near Fochville (Table 1), and west of Pretoria at Hekpoort, in discontinuous, up to one-meter high outcrops (Fig. 5i). In one case a thin lens could be followed circa 300 m along strike.

Whereas *Oberholzer and Eriksson (2000)* described fragment sizes in the range of 3 mm – 22 cm in the lapilli-tuff close to the Hekpoort river area, we only observed clasts smaller than 5 mm diameter (Fig. 5j), which suggest they are significantly more distal, if both belong to the same stratigraphic layer. The clast lithologies are either mafic, scoriaceous material or lithic fragments of mudstone and siltstone, or individual quartz grains arranged in graded beds, generally well-bedded and fining upward. Most of the finer clasts are quartz grains of moderately rounded to well-rounded shapes. The bigger lithic fragments often show bedding. All these fragments were probably derived from the underlying sediments of the Timeball Hill or Rooihoogte / Duitschland formations of the Pretoria Group (Fig. 2). The scoriaceous material (darker layers in Fig. 5j) is quite elongated and arranged along lamination planes, possibly resulting from flattening and welding. This fabric suggests a pyroclastic origin. The porosity appears to be very low in these rocks.

Massive lapilli-tuff and tuff-breccia

The massive lapilli-tuff and tuff-breccia (Fig. 5j, k), were found at the base of the Hekpoort Formation in the western part of Fochville, just south of Wedela, and in the eastern part of Pretoria, close to Mooikloof (Fig. 1; Table 1). Although both correspond to the lowermost deposits of the Hekpoort Formation, differences are observed. The Mooikloof volcanoclastic rocks are massive lapilli-tuffs, have clasts can reach 1cm in diameter and are rather similar in composition to the stratified lapilli-tuffs west of Pretoria. Their massive appearance, the absence of internal stratification, and, finally, the presence of partially devitrified volcanic glass shards and lava particles rather than scoriaceous material distinguish them from the massive lapilli-tuff and tuff-breccia close to Fochville.

The volcanoclastic rocks in the Fochville monocline (Table 1) range from massive lapilli-tuffs to tuff-breccias containing clasts of up to 20 cm in diameter (Fig. 5k). Lithic fragments are rare except for individual sub-rounded quartz grains, which occur in very low abundance (<2-3 vol%). Most of the clasts are of randomly oriented scoriaceous material (< 3 mm) and show ductile stretching. Larger clasts resemble bombs but are actually basalt fragments, quite often similar to flow-tops (Fig. 5l). The basaltic clasts show hypocrystalline textures with 1-2 mm long euhedral pyroxenes (lower part of Fig. 5j) fully pseudomorphosed by clinochlore and embedded in a matrix of randomly oriented plagioclase microliths. Although similar minerals can be found in other regions in outcrops of the Hekpoort Formation, the observed textures were not found elsewhere in the formation. The biggest clasts are generally highly weathered, but resemble volcanic bombs or reworked amygdaloidal flow top material. Finally, big angular blocks (up to 50 cm) of shale and siltstone, likely sourced from the underlying Timeball Hill Formation, occur occasionally. They highlight the high-energy character of deposition. *Lenhardt et al. (2012)* interpreted similar massive lapilli-tuff observed in the eastern Transvaal sub-basin as pyroclastic flow deposits. What we observed might be either the lateral extension of such large scale deposits, or it may be linked to more localized events.

Pyroclastic breccias

Pyroclastic breccias are the coarsest volcanoclastic rocks found in all the areas apart from the Hekpoort river region (Table 1). They were only found in the western part of Fochville (Table 1) just below the 30 cm thick laminated tuff deposits. The boundary between the two deposits is sharp. The pyroclastic breccias consist of unsorted to poorly sorted material containing particles that range in size from clay-sized to blocks of up to 15 cm in diameter (Fig. 4l); the biggest clasts are generally angular. Such deposits might correspond to the ‘volcanic diamictite' described by some authors (e.g., *Oberholzer and Eriksson, 2000*; *Lenhardt et al., 2012*).

The composition of clasts is the same as in the lapilli-tuff and tuff-breccia, but includes a notable concentration of fragments of limestone/dolomite, likely from the Malmani Subgroup. All such fragments show signs of reaction with the basaltic host lava. The material surrounding the lithic blocks is quite similar to massive lapilli-tuff, showing welding of scoriacious clasts, suggesting that this rock is a true pyroclastic deposit, contrary to the previous interpretation as coarse volcanic debris flows, possibly deposited by lahar processes (*Eriksson and Twist, 1986*; *Oberholzer and Eriksson, 2000*).

Lahars and related mass flow deposits in the Hekpoort River valley

Tuffacous beds with a very indistinct bedding delineated by weak alignment of clasts in a sandy matrix are found in the Hekpoort River valley (Fig. 1). The clasts are of varying composition, size and rounding. Very angular clasts of mafic lava and scoria and rounded clasts of fine-grained felsic lava are common and occur together with rare clasts of sandstone, quartz porphyry and shale. Some of the lava clasts exhibit reaction rims towards the matrix, whereby the matrix is mostly hardened but sometimes also weathering out, preferentially around the clast. This may indicate an incorporation of hot clasts into the wet mass flow directly from an ongoing volcanic eruption. The size of the clasts varies between <1 cm to 15 cm in diameter and increases to ca. 30 cm in diameter. The maximum clast size encountered is, however, a clast of massive lava of ca. 3 m in diameter (see Table 1 for coordinates). In general, the clasts seem to decrease in size towards NE and W, away from this location. Clast-supported deposits can be observed in this area, probably indicating more proximal deposition. Contrary to the pyroclastic breccias described above, the largest clasts in these mass flow deposits are usually well-rounded. The texture is matrix-supported, massive and lacks distinct layering. Only locally, clast-supported deposits can be observed further towards the SW, probably indicating more proximal deposition.

Locally, these mass flow deposits rest on aphanitic lava. A crude coarsening upward of the clasts was observed SW of Broederstroom (Fig. 1), where well-rounded clasts of up to 50 cm diameter can be found. The above deposits can be traced laterally for at least 8 to 12 km between Hekpoort and Sterkfontein (Fig. 1), where they were described by *Oberholzer and Eriksson (2000)*. We interpret these deposits as various lahar fans because of their large variety of clast compositions and sizes, whereby volcanic clasts of mafic lava clearly dominate the clast composition. Fig. 3b depicts the inferred geological setting of these deposits in a simplified sketch.

3.2.3. Paleosol and interbedded sedimentary units

Non-volcanoclastic sedimentary rocks are rarely encountered within the Hekpoort Formation. The most studied occurrence (firstly by *Button, 1973*) is the so-called "*Hekpoort Paleosol*", which has been used both *pro* and *contra* in the discussion of the early Proterozoic Great Oxidation Event (e.g., *Retallack and Krinsley, 1993*; *Ohmoto, 1996*; *Holland et al., 1997*; *Beukes et al., 2002*; *Ohmoto, 2004*; *Retallack et al., 2013*).

Outcrops east of Pretoria contain lenses of meter-thick, silicified (cherty) shales, which contain layers of iron-oxide/hydroxide and siltstones occurring over tens to hundreds of meters laterally (Fig. 5n, o). At one locality (Mooikloof, Table 1), one such lens developed in a small synclinal structure displays imprints interpreted to originate from raindrops. The cherty texture may be a result of contact metamorphism related to the overlying lava flow or sill. The contact margin in the overlying lavas is characterized by brecciation, also present in the finely laminated sedimentary rock, and vesicles. This implies intrusion into a wet sediment, and may thus be close to the time of sediment deposition. The outcrops display small kink folds and micro-faulting at outcrop (Fig. 5n), as well as at thin section scale (Fig. 5o). These structures are possibly a result of slip between surrounding lava flows and the sedimentary rock during the flexural tilting and formation of the shallow, E-W striking and westerly plunging syncline that might be related to the emplacement of the Bushveld Complex.

3.2.4. Structures possibly linked to subaqueous extrusion

Previous studies have interpreted the Hekpoort lavas as mainly subaerial extrusives (*Button, 1973*; *Lenhardt et al., 2012*), although the occurrence of open water bodies such as localized ponds and lakes during Hekpoort volcanism was proposed by *Button (1973)*, who described interbedded epiclastic sedimentary rocks, displaying cross-bedding and cross-lamination, and suggested deposition in subaqueous environment. Apart from the obvious presence of shales, we propose that the following observations support local subaqueous environments.

Hyaloclastites

Hyaloclastites and structures resembling pillows were found at the top of the Hekpoort Formation only in the Potchefstroom area (Table 1), in proximity to outcrops of the Dwaalheuwel/Strubenkop formations (Fig. 5p, q). The putative pillows are highly weathered and thus inconclusive, however, the presence of hyaloclastites is more convincing (Fig. 5p). Polished sections reveal a texture composed of rounded fragments rich in amygdales and surrounded by brecciated clasts in an aphanitic texture, sometimes containing euhedral pyrite (1-4 mm diameter). The amygdales are heterogeneous in shape, distributed unevenly in the rounded fragments, and display mineralogical infill different from amygdales in other parts of the Hekpoort. The majority of these fillings represent tiny quartz geodes. These rounded fragments can have sizes greater than 10 cm and can contain amygdales of up to 2 cm in diameter. Several of the analyzed fragments also showed pervasive alteration, interpreted as early palagonitization (Fig. 5q). Palagonitization was not found in any other Hekpoort rocks.

Variolitic lava flows

Variolitic lava flows, of up to 30 m in thickness and over 1 km of strike, can locally be found at the basal portion of the Hekpoort Formation near Fochville, around and in the town of Wedela (Table 1; *Humbert et al., 2017*; *Humbert et al., in revision a, b*). These flows present at least two distinct layers per flow. The upper one is rich in varioles, in a fine-grained magmatic groundmass. The concentration of varioles is quite constant in any particular layer but differs between successive flows. The diameter of individual varioles ranges from one to ten centimeters (Fig. 5r) (*Humbert et al., in revision a*). Coalescence can sometimes be observed among the biggest varioles (Fig. 5r). The varioles are composed of radially oriented acicular clinopyroxene needles (with a width of 1 μm). The interface between varioles and the groundmass can be marked by a succession of diffusion rims showing alternatively brighter and darker colors than the varioles (top-left of Fig. 5r; dark rim followed by a brighter rim in Fig. 5s). The variolitic lava flows are also rich in skeletal clinopyroxene phenocrysts (30-70% of the rock), which are randomly oriented and homogeneously distributed throughout varioles and groundmass (Fig. 5s).

Humbert et al. (2017) interpreted these structures as being related to a complex process of super-cooling whereby the skeletal clinopyroxenes were formed first, followed by acicular clinopyroxene, thereby defining the varioles, and provoking diffusion of several elements that poorly fit into the clinopyroxene lattice (*Gardner et al., 2014*) Finally, the remaining glass underwent devitrification, forming the finely crystalline matrix observed as the groundmass.

In the absence of physical or chemical evidence for carbonate-rich xenoliths that could cause fast cooling (e.g., *Deegan et al., 2010*) in these variolites, it seems more likely that water was the cause of the inferred supercooling, suggesting that the variolitic lava flows were extruded subaqueously (*Humbert et al., in revision a*).

4. Petrology

The majority of the Hekpoort lavas exhibit aphanitic (sample DK) to hypocrystalline (samples GCEE and DTHB) textures (Fig. 4e). The maximum degree of crystallinity was found in the outcrops west of Potchefstroom (sample PWD; see table 2 for location). These rocks display microlitic textures marked by randomly oriented centimeter-scale plagioclase laths in a hypocrystalline matrix containing skeletal plagioclase (Fig. 6c) and amygdales. Whereas all other Hekpoort samples are clearly lavas, such rocks could be shallow intrusives, and, in the absence of evidence for crosscutting relationships, most likely a sill. The geochemistry of sample PWD is indistinguishable from other samples of the Hekpoort Formation (see section 5).

Petrologic study confirms that all the samples experienced low-grade greenschist facies metamorphism, in addition to metasomatic alteration that is principally marked by silicification, K-metasomatism (*Reczko et al., 1995; Coetzee, 2001)* and albitization. Primary minerals are still preserved, mostly clinopyroxenes (Fig. 6c to f), which are mainly Mg-rich augite, together with diopside ± pigeonite in some samples (Fig. 7a). Samples with the highest Mg# (i.e., Mg# > 60; see section 5) contain pigeonite and augite, while augite or diopside occur in the more differentiated samples. Augite, when present, displays Fe-rich rims. The geothermometry based on the couple pigeonite – augite indicate a crystallization temperature ~1200 -1000°C (Fig. 7b) based on the pyroxene phase diagrams at 5kb by *Lindsley (1983)*. Similarly, the augite rims crystalized at a temperature of ~1100 - 800°C, based on phase diagrams at 1 atm, from the same author (not shown).

Some relics of primary igneous minerals can be identified. Pyroxenes fully pseudomorphosed by clinochlore or actinolite (Fig. 6d) have been interpreted as orthopyroxene. Microliths of Mg-rich hornblende are rarely found in some samples, but never in abundances of more than 1%.

Plagioclase can be present as 0.8 - 1.2 mm wide phenocrysts (Fig. 4e) or as 0.5 - 1 mm euhedral grains (Fig. 6b), but most commonly it is present as acicular crystals (Fig. 6a). Microprobe data obtained on eight plagioclase crystals reveal that they are all labradorite (An_{52-68}, average An_{62}), in agreement the observations by *Crow and Condie (1990)*. Most of the plagioclase has been albitized, and the Ca released formed secondary calcite (Fig. 6c), epidote (Fig. 6b) and, rarely, titanite. Some plagioclase crystals are also partly replaced by sericite and K-feldspar. The only other true primary mineral preserved in the lavas is magnetite identified through magnetic mineralogy studies by *Humbert et al. (2017*).

Other secondary minerals observed are almost pure K-feldspar and quartz. The latter is the main mineral filling the amygdales, but quartz is also found around ferromagnesian minerals (bottom-right of Fig. 6d). The other minerals filling amygdales are clinochlore, calcite and, less common zeolites.

We have also studied samples from the Ongeluk Formation (see section 5) which are all aphanitic in texture. Only pseudomorphs after pyroxene and plagioclase, consisting of chlorite, with minor actinolite, epidote and tiny patch of quartz were observed, all with similar compositions to their equivalents in the Hekpoort Formation.

5. Geochemistry

Major and trace element contents were determined in 16 samples of the Hekpoort lavas obtained from all studied areas, as well as 12 samples of the Ongeluk Formation taken for comparison in the Griqualand West sub-basin in five areas distributed around Postmasburg

(Table 2). The selected samples were either very poor in amygdales, or the latter were manually separated before crushing in a jaw crusher. A representative split was milled using an agate mill. Element contents were determined at ACME Labs, Canada; major elements were analyzed by X-ray fluorescence spectrometry on glass beads prepared from powdered whole-rock samples with a sample-to-flux (lithium tetraborate) ratio of 1:10. Volatiles were determined by loss on ignition. Precision for the different elements is better than ± 1% of the reported values. Trace elements were analyzed using inductively coupled plasma mass spectrometry (ICP-MS) in the same laboratory. The sample powders were dissolved in lithium metaborate flux fusion and the resulting molten bead was rapidly digested in weak nitric acid solution. The precision and accuracy for each element are given in Table 2.

5.1. Metasomatic alteration and weathering

Due to the likelihood of alkali and silicon mobility during metamorphism or metasomatic alteration, the Zr/TiO_2 versus Nb/Y plot (Fig. 8a) is preferred to the more traditionally used TAS diagram (Fig. 8b). The constant SiO_2 content versus the evolution of Mg number (Mg# = molar [MgO/(MgO + FeO*)]) strongly suggests that the Hekpoort and Ongeluk samples were affected by silicification (Fig. 9). Although silicification inevitably also affects concentrations of other elements, ratios, such as the magnesium number will not be influenced to the same extent. We therefore used Mg# as a differentiation index in Fig. 9. The increase of Zr in function of Mg# (Fig. 9) supports the idea that Mg# can be used as a proxy for differentiation. The scatter of both Na_2O and K_2O in Figs. 8b and 9 strongly suggest that these elements have been affected by alteration too.

Regarding the effects of weathering, the chemical index of alteration (CIA = molar $[Al_2O_3/(Al_2O_3 + CaO + Na_2O + K_2O)] \times 100$) (*Nesbitt and Young, 1982*) measures the extent to which feldspars have been converted to aluminous clays. For unaltered basaltic rocks, CIA values range from 30 to 45. CIA values range from 41 to 54 (Hekpoort) and from 37 to 44 (Ongeluk) while clays are characterized by CIA values above 75. This thus suggests that the samples were not intensively altered. The notable loss on ignition (LOI) of the samples is attributed to their high chlorite content. This LOI is fairly constant relative to Mg#, between 2.5 to 3.7 wt%; only some samples with Mg# > 58, which were possibly richer in ferromagnesian minerals, and one Ongeluk pillow lava sample, show values above 4 wt% of LOI.

Fig. 8a shows that all Hekpoort and Ongeluk samples plot in the basalt field, but close to the boundary with the basaltic andesite field. Because of the high MgO content of the Hekpoort and Ongeluk samples, between 5.0 and 11.3 wt% (mean: 7.0 ±1.7 wt%; 50 < Mg# < 69) and 5.2 and 8.2 wt% (mean: 6.0 ±0.8 wt%; 50 < Mg# < 56) respectively, it seems most appropriate to classify the Hekpoort and Ongeluk rocks as basalt.

5.2. Crystal fractionation inferred from geochemistry

We have estimated the extent of fractional crystallization for the Hekpoort Formation by using the Rayleigh Equation which can be reduced to $F = C_0/C_L$ for highly incompatible elements, with C_0 representing the initial concentration of an element in the parental or less differentiated melt, C_L is the concentration in the residual liquid and F is the fraction of melt. We calculated F based on Th; we prefer Th over Cs, Rb and Ba which are nominally more incompatible but also quite fluid-mobile. Using the Th value of the sample with the highest Mg# (i.e., ≈ 69) for C_0 and an average of the 4 samples with the lowest Mg# (i.e., between 54 and 50) for C_L, we obtained F = 0.58 and thus 42% of crystal fractionation for the Hekpoort Formation. F is 0.97 for the Ongeluk samples, as, their Mg# values are mostly rather low, of 55 to 51 only.

As previously detailed, metasomatism and element mobility occurred in the Hekpoort lavas; thus, the content of mobile elements (Si, Na, K, potentially Ca, large-ion lithophile elements) may not be representative of magmatic values. The exact identification of fractionating mineral assemblage of the Hekpoort lava is therefore complicated to constrain through the geochemistry.

The decrease of Cr and Ni with decreasing Mg# (Fig. 9) respectively suggest a fractionation of pyroxenes and / or olivine and / or Cr-spinel (Cr). A break in slope is actually observed in the two plots at Mg# = 55, notably in the case of Ni versus Mg#, implying that pyroxenes and / or olivine fractionated from the parental magma until its Mg# decreased to 55. By recalculating F for each interval and using the fractional crystallization, we obtained D_{Ni} = 3.5 and D_{Cr} = 4.9 in the Hekpoort Formation lavas. It mostly suggests a fractionation of pyroxenes and chromite, possibly together with minor olivine as the D_{Ni}(estimated) values are 14, 5 and 7 and D_{Cr} values 0.70, 10 and 34 for olivine, Opx and Cpx respectively (*Rollinson, 1993*). Sc is compatible in pyroxene, especially Fe-rich clinopyroxenes in which Sc^{3+} substitutes for Fe^{3+} (literature data on basalt from GERM website: https://earthref.org). The Sc contents is somewhat scattered, possibly related to the fractionation of different pyroxenes with different content of Fe^{3+}. We obtain a D_{Sc} = 1.67 (between the samples with the highest and the lowest Mg#) again suggestive of pyroxene fractionation (D_{Sc} = 1.7), possibly in conjunction with olivine (D_{Sc} = 0.28) (literature data on basalt from GERM website: https://earthref.org). Chromite was also observed in one Hekpoort sample (Mg# = 59) and this mineral may explain most of the Cr decrease.

The increasing content of Dy with decreasing Mg# argues against amphibole fractionation (*Davidson et al., 2007*). Similarly, the increase of TiO_2 with decreasing Mg# shows that (titano-)magnetite did not fractionate from the magma. Finally, the case of plagioclase remains complex, because most of its constituents are mobile (i.e., Si, Na, Ca, Ba, Sr). However, the increase of Al until Mg# = 55, followed by a slight decrease, indicates that plagioclase only started crystallizing at a more advanced stage of differentiation.

5.3. Trace elements patterns

Fig. 10 presents the chondrite (Cl) normalized rare earth element (REE) (a, b) and primitive mantle-normalised multi-element (c, d) patterns of Hekpoort and Ongeluk samples, respectively. All samples show (1) a strong enrichment of light REE values relative to heavy REE ($(La/Lu)_N$ = 7-10), (2) remarkable homogeneity of the trace element patterns for the samples of each formation, with just a slight scattering of the HREE for the Ongeluk samples, and (3) strong similarities between the two formations.

The two formations both have clear negative anomalies for Ba, Nb - Ta, P and Ti, positive for U, and variable for Eu, K and Sr but mainly negative for the latter element. The variable anomalies in K and Sr are likely linked to the high mobility of these elements as its contents scatter widely independently of the Mg# of the samples. Similarly, Eu^{2+} can also be mobile, but from the limited variability of Eu/Eu* versus Mg# (Table 2) we infer that this has not been the case here. The negative Eu and Ti anomalies could be interpreted as fractionation of plagioclase and titaniferous magnetite, respectively, from the primary magma. This is however in disagreement with the overall increase of TiO_2, Al_2O_3 (and also CaO and Na_2O, even though these elements are mobile) with decreasing Mg# (Fig. 9). The Sr anomalies are also variable, which can be related to the high mobility of this element. These three anomalies can also be inherited from the mantle source. The constant Eu/Eu* versus Mg# supports the last hypothesis. Another possibility would be an earlier stage of crystal fractionation (of plagioclase and titaniferous to explain the Eu- and Ti-anomalies), but this seems unlikely as higher pressures do not favour plagioclase crystallization.

Finally, negative Eu, Nb, Ta and Ti anomalies are typical of arc signature in Phanerozoic mafic rocks (e.g., *Elburg, 2010*) and of crustal input in general (*Pearce, 2008*). An arc signature implies a positive Sr-anomaly which is not observed in the Hekpoort and Ongeluk samples. The possibility of metasomatism of the mantle source by continental crust will be discussed below (section 6.3).

6. Discussion

The Hekpoort Formation lavas can be compared to Phanerozoic basalts concerning the physical volcanology; the formation *inter alia* also contain various volcanoclastic rocks, hyaloclastites, pahoehoe flows and vesicle cylinders and the intercalated sedimentary rocks. Geochemically, this formation resembles the Ongeluk Formation which is ca. 200 myr older. The long time span separating the two formations can provide information about the source (possibly being the within the cratonic lithosphere) and the evolution of the Hekpoort magma. This is discussed below.

6.1. Metamorphism and metasomatism

The presence of secondary minerals such as chlorite, quartz, alkali feldspar, sericite, zeolites, epidote, carbonates, titanite and pyrite in the Hekpoort Formation rocks shows that they were subjected to both low-grade metamorphism and metasomatism. The chlorite, being the most common mineral in the Hekpoort and Ongeluk lavas, explains their notable LOI whereas they do not present obvious evidence for strong alteration macroscopically. The mineral assemblages (epidote + actinolite + chlorite + albite) in the majority of Hekpoort lavas reflect peak metamorphic conditions no higher than greenschist facies (*Button, 1973*; *Coetzee, 2001*; *Lenhardt et al., 2012*), akin to the rest of the Transvaal Supergroup (*Button, 1973*; *Miyano and Beukes, 1984*).

It is nevertheless complicated to estimate the exact metamorphic facies the Hekpoort lavas were subjected to as the secondary minerals did not all appear simultaneously. For instance, the chlorite is present as a pseudomorph of ferromagnesian minerals, but also in the mesostasis, probably linked to devitrification of volcanic glass (e.g., *Frey, 1987*). In addition, most of the secondary minerals can have a pre-metamorphic origin, as they are also typical of hydrothermal alteration of basalts (e.g., *Best, 1992*; *Shelley, 1993*). These rocks may also have undergone alteration in a sub-aqueous setting, especially in the upper part of the succession, but certainly experienced more than one episode of alteration. Quartz is present as infilling of amygdales but also as scattered micro-grains, probably due to silicification. Silicification has been observed in other Paleoproterozoic mafic rocks in the Kaapvaal craton; for instance, *Wabo et al. (in press)* noted that clinopyroxene crystals were preferentially silicified compared to plagioclase in a weakly altered gabbroic dyke dated at 1871 ± 5 Ma. Several generations of silica mobility including the near surface, deep, pervasive silicification within few tens to hundreds of meters below the African Surface (Upper Cretaceous to Neogene) are known from all rocks of the Kaapvaal Craton (*Burke and Gunnell, 2008*; *de Wit et al., 2009*; *Partridge and Maud, 2014*). The observed micro-grains of quartz can also result from silica remobilization during metamorphism (i.e., without metasomatism); for instance, chlorite contains less silica than pyroxenes. Yet, the roughly constant silica content with varying Mg# suggest that a certain threshold of silica content was reached in the Hekpoort and Ongeluk rocks and argues in favor of Si-metasomatism, mostly in the less differentiated samples. But, the extent of this metasomatism on the Hekpoort lavas remains unknown. *Coetzee (2001)* noted intergrowths of quartz with K-feldspar, and proposed that silicification and K-metasomatism were coeval. However, the alkali content is quite variable (Fig. 8b), most obviously so in the Ongeluk samples with an alkali content between 1 to 4 wt% for similar SiO_2 values. Alternatively, both the Hekpoort and Ongeluk lavas could be anorogenic boninites, also called boninitic-noritic (BN) rocks, which are common during the 2.5–2.1 Ga period and have a SiO_2 > 52 wt% (Srivastava and Ernst, 2013; Ernst, 2014), in which case their relatively high silica content is primary (see discussion below).

Another complexity is that, in addition to the metasomatism and burial metamorphism during more than 2 billion years of history, the Hekpoort lavas were also at least partly subjected to impact (shock) metamorphism (the Vredefort Impact Structure) and to several episodes of contact metamorphism which probably induced mineralogical changes. During paleomagnetic studies done on Hekpoort rocks from the same study area, *Humbert et al. (2017)* characterized remanent components linked to the Bushveld Complex (2.054 Ga), the Karoo LIP (~0.18 Ga), and possibly the Umkondo LIP (~1.1 Ga). Nevertheless, metamorphism in the Hekpoort Formation, which was not totally pervasive because clinopyroxenes are still party preserved, was mainly related to burial. No dynamo-metamorphic fabrics, such as schistosity, foliations and mineral lineations, were observed in the rocks.

6.2. The Hekpoort and Ongeluk basaltic formations

In figure 9, the Ongeluk samples fall on the low-Mg# extension of the Hekpoort trends, as already observed by *Cornell et al. (1996).* The Hekpoort and Ongeluk patterns also show substantial overlap in the multi-element diagrams (Fig. 10c, d); the main differences relate to the Th and U contents, which are slightly higher in the Hekpoort Formation (Th = 8.35 ± 1.64 ppm; U = 3.23 ± 0.58 ppm) than in the Ongeluk Formation (Th = 5.78 ± 0.48 ppm; U = 1.40 ± 0.23 ppm). Note that *Schütte (1992)* obtained higher values for both Th (i.e., 6.65 ± 1.75 ppm) and U (i.e., 2.32 ± 0.60 ppm) for a larger set of Ongeluk samples (104 samples; Fig. 9), but the fact that the data were acquired by XRF may cast some doubt on their accuracy due to their low concentration in the lavas. Two other differences can be noted: slightly higher Sc and P_2O_5 contents in the Ongeluk Formation (Fig. 9). The concentrations of the latter remain very low in both formations and the offset in Sc might be explained by slight differences in degree of fractionation or the composition of clinopyroxene between the two formations.

Most studies on the Hekpoort and Ongeluk lavas relate these rocks to basaltic andesites (e.g*., Button, 1973 Engelbrecht, 1986*; *Oberholzer, 1995*; *Cornell et al., 1996; Lenhardt et al., 2012*) or andesites (*Sharpe et al., 1983*; *Crow and Condie, 1990*; *Harmer and von Gruenewaldt, 1991*; *Oberholzer and Eriksson, 2000*), but Fig. 8a demonstrates that all samples plot as basalts, although close to the boundary with the basaltic andesite field. Although the high SiO_2 contents (average of 54.5 ± 1.1 wt% and 54.25 ± 2.8 wt% for Hekpoort and Ongeluk samples, respectively) suggest that these samples are too silica-rich to be basalts, the high MgO content (5 - 11 wt%) of both the Hekpoort and Ongeluk contradicts this interpretation. High-Mg andesites (with MgO > 6 wt% and SiO_2 > 54 wt%; *Wood and Turner, 2009*) can also fit such characteristics but these seldom contain plagioclase crystals (*Shellnutt and Zellmer, 2010*) as the Hekpoort lavas do. Other igneous rocks with high MgO and high SiO_2 contents are (orogenic) boninites (*Gill, 2010*), which however are characterized by lower concentrations of TiO_2 (< 0.5 wt%) and Zr (typically largely below 100 ppm).

In the previous section, we mentioned that the Hekpoort and Ongeluk formations lavas could potentially be anorogenic boninites (or BN suite rocks), which, like orogenic boninites, contain high SiO_2 (>52 wt%), high MgO (>8 wt%), and low TiO_2 (mostly < 0.5 wt%) (*Smithies, 2002*; *Srivastava, 2008*). Based on Al_2O_3/CaO ratios, Hekpoort and Ongeluk formations would be classified as low-Ca anorogenic boninites that show geochemical characteristics similar to high-Mg norites (*Srivastava, 2008*). The two formations share several similarities with the BN suite rocks: (1) most of the samples have SiO_2 > 52 wt%; (2) they plot in the field of high-Mg norites in the TiO_2 vs Zr diagram of *Smithies (2002)* but not in the fields of SHMB (siliceous high magnesium basalts) assumed to be volcanic rocks related to BN rocks (*Srivastava and Ernst, 2013*; *Ernst, 2014*); (3) they were emplaced during the period of 2.5–2.1 Ga like most BN suites in the world (*Srivastava, 2008*; *Srivastava and Ernst, 2013*; *Ernst, 2014*). However, the TiO_2 and MgO contents of most samples are higher than 0.5 wt% and notably lower than 8 wt%, respectively. In the 18 worldwide examples of average chemical compositions of BN suites from *Srivastava (2008)*, most show MgO values > 10 wt%, with an average of MgO = 13.2 wt% and higher Mg# (i.e. > 63 with an average of 70.3 ± 4.5) and are thus less differentiated than the Hekpoort and Ongeluk formation lavas. If we only consider the 5 Hekpoort Formation samples with Mg# > 60 (table 2), they present MgO values from 7.5 to 11.3 wt%, which is more in agreement with BN rocks, although TiO_2 values are higher than 0.5 wt%.

In the MgO vs SiO_2 diagram for distinguishing the boninite – high-Mg andesite series from the basalt – andesite – dacite – rhyolite series (*Pearce and Robinson, 2010*; *Ernst, 2014*), two-thirds of the Hekpoort and Ongeluk samples plot in the transition zone between the two fields. In both series the SiO_2 is assumed to increase with decreasing MgO, while we observe a fairly constant SiO_2 content in all the samples (Fig. 9). The Hekpoort and Ongeluk formations could equally well be interpreted as basalts or basaltic-andesites subjected to silicification, an interpretation supported by the quartz micro-crystals disseminated throughout the lavas. This is not surprising for lavas older than 2 Ga, surrounded by siliciclastic formations (Fig. 2). Yet, the extent of silicification remains unknown; it is possible that it was low in the most differentiated samples. The partition coefficient calculated from the evolution of both Cr and Ni during differentiation (see section 5.2) shows that pyroxenes rather than olivine were the dominant fractionating phase, which might mean that the lavas were saturated in silicon, which suggests a greater affinity to basaltic andesites than basalts. However, olivine is typically also an important constituent of basaltic andesite (e.g., Gill, 2010). Its relative low abundance within the fractionating minerals, would then be more typical of a more evolved magma type. Moreover, some ultramafic rocks, for instance komatiites, can sometimes mostly or uniquely contain pyroxenes which are generally Mg-rich (e.g., Arndt and Fleet, 1979). We however did not observe any preserved orthopyroxene in the Hekpoort and Ongeluk lavas. Another possibility is that olivine mainly fractionated from the primary melt at an earlier step, giving the parental melt from which the lava erupted. Plagioclase in the Hekpoort Formation is labradorite (at least in sample with Mg# > 55), highlighting that most of the lavas are basalts rather than basaltic andesites, which generally contain more albite-rich plagioclase (typically andesine*; Gill, 2010*).

Although the observed volcanoclastic rocks such as block-and-ash flow deposits, which are only a minor constituent of the Hekpoort Formation, are mostly restricted to magmas of andesitic to dacitic compositions (e.g., *Cole et al., 2002*; *Saucedo et al., 2002*; *Busby et al., 2004*), basaltic block-and-ash flows have also been described (e.g., *Kobayashi et al., 2003*; *Miyabuchi et al., 2006*).

In conclusion, the different arguments presented here show that the Hekpoort and Ongeluk lavas are probably not andesites, but either basaltic andesites, basalts or possibly evolved anorogenic boninites. The Zr/TiO_2 *vs.* Nb/Y coupled with the high MgO content, the high Mg#, and the labradoritic plagioclase, argue in favor of the Hekpoort lavas being basalts. The absence of olivine in the samples and the SiO_2 content (if we neglect impact of silicification) are more typical of basaltic andesite. Regarding the number of arguments, we will call the Hekpoort and Ongeluk lavas basalts.

6.3. The Hekpoort flood basalt formation

The 2324 ±17 Ma Timeball Hill Formation (*Dorland et al., 2004*) is regarded as an ancient deltaic complex (*Button, 1973*; *Eriksson et al., 2006*). The upper part of the formation, predominantly composed of either shale or siltstone, is directly and unconformably overlain by the Hekpoort lavas in the Potchefstroom area. Unlike the subaqueously deposited Timeball Hill rocks, the Hekpoort Formation was described as being largely deposited in a subaerial setting (e.g., *Visser, 1969; Button, 1973*; *Sharpe et al., 1983*; *Engelbrecht, 1986*; *Eriksson and Twist,* *1986*; *Oberholzer, 1995*; *Reczko et al., 1995*) and is seen as a major continental flood basalt event on the Kaapvaal craton (e.g., *Reczko et al., 1995*; *Cornell et al., 1996*). Our observations are in agreement with the previous studies. We noted the absence of wide-spread pillow lavas, or hyaloclastites in the studied areas. By contrast, we observed the presence of pahoehoe and flow tops composed of uniform amygdales layers (Fig. 4f), as well as a small area of bedding plane with preserved syn-depositional raindrop imprints (*Altermann et al., in preparation*), which are clear evidence for subaerial deposition.

Localized ponds and lakes (*Button, 1973*) can explain (1) the hyaloclastites (and possible pillows) at the top of the Hekpoort Formation lavas in the Potchefstroom syncline; (2) the variolitic lava flows at the lowermost part of the formation in the Hekpoort river valley; (3) the volcanoclastic rocks, which mostly result from phreatomagmatism, at the base of the formation in the studied areas.

Oberholzer (1995) estimated that volcanoclastic rocks and lava flows occur in approximately equal proportions in the southwestern part of the Transvaal sub-basin whereas several previous studies support a preponderance of lava flows in the whole Hekpoort Formation (*Button, 1973*; *Sharpe et al., 1983*; *Engelbrecht, 1986*; *Schreiber, 1991*). We observed that volcanoclastic rocks occupy a small portion of the formation in the areas we studied, in agreement with *Coetzee (2001)* for the area south of Potchefstroom. In summary, volcanoclastic rocks in the Hekpoort Formation are mainly confined to its basal portion and remain a minor rock type. Yet, the presence of large amount of volcanoclastic rocks in some localities (e.g., the Hekpoort River Valley, Fig. 3b) suggest that the Hekpoort magma chamber was rich in volatiles and/or that the lava encountered fluids at shallow surface (e.g., *Fisher and Schmincke, 1984*), thus promoting a more explosive style of volcanism and allowing the formation of varying proportions of lava flows and pyroclastic rocks.

The Hekpoort river area is in a way anomalous because it contains mainly coarse volcanoclastic deposits and mass flow deposits of lahars and coarse tuffs (*Oberholzer and Eriksson, 2000*; *this work)*. In places, the NE striking strata are oriented partly sub-vertical, with evidence for folding and faulting, but without any schistosity. Areas with subhorizontal bedding appear to be separated by normal faults from steeply dipping blocks of regional extent. We therefore envisage the development of a paleo-graben valley during the subsidence of the Kaapvaal craton that experienced stretching perpendicular to graben shoulders (*Eriksson et al., 2006*). Mass flows were triggered by earthquakes, accompanied by volcanic eruptions which led to the accumulation of thick and laterally extensive fans of coarse to fine, proximal to distal volcanoclastic deposits (Fig. 3b).

This extensional event was likely the underlying cause for Hekpoort magmatism. The more distal pyroclastic deposits in other regions as described above were likely associated with similar settings at different localities that still need to be found and mapped in detail. Similar processes were discussed for e.g., the Ventersdorp LIP lavas by *van der Westhuizen (2006)*, *Altermann and Lenhardt (2012)* and *Humbert et al. (in revision b)*.

6.4. Tectonic context and origin of the magma

The Hekpoort and Ongeluk magmas resemble subduction-related lavas in terms of their trace element patterns (*Harmer and von Gruenewaldt, 1991*; *this work)*. The only property that sets those magmas apart from real subduction-related magma in terms of major elements is their, on average, lower Al_2O_3 content, at similar MgO content (Fig. 11). The higher alumina content of subduction-related magmas is related to the presence of water in arc magmas that suppresses the early crystallization of plagioclase, thereby enriching the more evolved melts in alumina (*Green and Ringwood, 1968*; *Elburg, 2010*). This characteristic can be used to distinguish between true arc basalts and tholeiitic continental flood basalts, if rocks from unknown tectonic settings are studied (e.g., *Elburg and Goldberg, 2000*). The Hekpoort and Ongeluk magmas plot within the range of Karoo LIP magma, which also show clear resemblance with the subduction-related magmas, especially for the low-Ti Karoo magma resulting from shallow melting in the mantle (*Elburg and Goldberg, 2000*; *Jourdan et al., 2007*). Yet, the Karoo LIP magmas are not related to a subduction context but to the breakup of Gondwana. Equally, no evidence of a subduction during deposition of the Transvaal Supergroup is present; instead the tectonic setting of the Hekpoort lavas and the whole Pretoria Group, was inferred by *Reczko et al. (1995)* and *Eriksson et al. (2005)* to be in a rift-to-intracratonic-sag-type basin. This interpretation is in agreement with the local graben-like structure at the base of the Hekpoort Formation (Fig. 3), although this structure is of a small scale compared of the extent of the Hekpoort Formation; larger scale rifting around 2.23 Ga is still need to be confirmed. Finally, the large extent of the formation and its emplacement roughly in the center of the craton (Fig. 1) do not fit a subduction context, and confirm that the Hekpoort Formation represents within-plate magmatism.

Regarding the origin of the magma, some authors (e.g., *Lenhardt et al., 2012*) have interpreted the Hekpoort volcanics as mantle plume-related continental flood basalts, documenting processes within a replenished, fractionated, tapped, assimilated (RFTA; *Arndt et al., 1993*) magma chamber (*Reczko et al., 1995*). The RFTA model involves an asthenospheric source, replenishing and tapping of the magma chamber and contamination of the primary partial melts by crustal material accompanied by fractional crystallization. On the other hand, *Myers et al. (1987)* and *Harmer and von Gruenewaldt (1991),* concluded that the Hekpoort and Ongeluk magmas were formed by partial melting of a metasomatized subcontinental lithospheric mantle (SCLM), similar to other 3.0 – 2.1 Ga mafic igneous rocks (*Myers et al., 1987)*. For *Harmer and von Gruenewaldt (1991)* the subduction-type signature reflects the involvement of a lithospheric source generated through subduction processes at the time of crust formation, i.e., inheritance of an older subduction signature recorded in the SCLM. We envisage the last hypothesis as the most likely one.

With respect to the RFTA model, the data presented here indicate a role for fractional crystallization of olivine, pyroxene ± plagioclase, leading to evolved Mg#, increasing incompatible and decreasing compatible element contents. The source of the magma is more difficult to elucidate, as the characterization of many mantle reservoirs is based on ratios of mobile trace elements (e.g., U/Pb, Rb/Sr) or radiogenic isotope ratios, for which data are scarce. The $^{147}Sm/^{144}Nd$ ratio, based on two elements less sensitive to alteration, give mean values of 0.116 ± 0.007 and 0.117 ± 0.006 for the Hekpoort and Ongeluk formations respectively, not to mention that they match with to the $^{147}Sm/^{144}Nd$ values measured by *Cornell et al. (1996),* for the Ongeluk samples. *These authors* calculated an average εNd of +0.9 for the Ongeluk Formation. The mean value was obtained using the 2222 ± 12 Ma age of Ongeluk Formation. Using the more recently determined 2426 ± 3 Ma age of the Ongeluk Formation (*Gumsley et al., 2017*), the εNd is ~ +3.0. This value is indistinguishable from the depleted mantle value at that time (~ +2.7; *DePaolo, 1988*) and it clearly indicates that the Ongeluk primary magma did not experience significant crustal contamination. For the Hekpoort lavas, $^{143}Nd/^{144}Nd$ data are unfortunately lacking. It should be noted that the REE pattern of the Ongeluk Formation (Fig. 9c), showing a strong enrichment of light over heavy REE, is not really in agreement with a depleted mantle source for the Ongeluk Formation, unless mantle re-fertilization took place shortly before eruption.

The Th/Yb versus Nb/Yb diagram (Fig. 12a) shows that both the Hekpoort and Ongeluk Formation have high Th/Nb values, plotting in the area of crustal material and far away from the MORB (DM) – OIB range.

High Th/Nb values can in theory be explained by crustal contamination of magma originating from the depleted mantle (Fig. 12b), but this disagrees with the positive εNd values of the Ongeluk lavas. In addition, according to the parameters used in the models (see the figure caption), it would require 90% of crystal fractionation. Another option is a direct derivation from a mantle component that was metasomatised by incompatible element-enriched melts or fluids from a subducting slab. According to the SZC model presented in Fig. 12c, the Hekpoort and Ongeluk magmas would require an important input of subduction zone material to the mantle source, to reach their Th/Nb values. It also indicates that the mantle source is most likely to already have been moderately enriched prior to addition of the subduction zone material. To produce high Th/Nb magmas such as the Hekpoort and Ongeluk from a source within asthenospheric mantle, only a very small degree of partial melting would permit significant enrichment of Th over Nb, unless Nb was withheld in the source by a specific mineral phase. Plume-related magmas typically have high Nb and Th, and are therefore not a source for high Th/Nb magmatism.

To sum up, our data do not permit to identify unequivocally the source of the Hekpoort and Ongeluk primary magmas. Nevertheless, both formations (1) display similar high Th/Nb values, (2) show LREE / HREE enrichment, suggesting either an enriched source or a low degree of melting from the source, (3) have negative Nb, Ta and Ti anomalies, similar to present-day subduction components or continental crust, and (4) do not show isotopic evidence for crustal contamination (at least in the case of Ongeluk Formation).

6.5. Implications of Hekpoort-Ongeluk 'equivalent' geochemistry

The comparison between Hekpoort and Ongeluk samples demonstrates that the two formations are geochemically very similar (Figs. 8 to 10), which could point to a common source. *Myers et al. (1987),* based on the comparison of trace elements on 13 volcanic sequences from the Kaapvaal Craton between 3.0 – 2.1 Ga, concluded that all the volcanic rocks show 'uniform behavior' of trace elements during this period, related to a common origin (i.e., metasomatized SCLM), but this conclusion was based on the comparison of only 2 major (Ti and P) and 5 trace elements (Nb, La, Ce, Zr, and Y). Even though Nb and P show similar behavior, the full REE and incompatible element diagrams show significant differences (Fig. 13). The similarity between the 2224 ± 21 Ma (*Burger and Coertze, 1973)* Hekpoort Formation and the 2426 ± 3 Ma (*Gumsley et al., 2017*) Ongeluk Formation is actually a conspicuous exception.

The Hekpoort and Ongeluk formations show positive U and Th anomalies, and relative high contents of those two elements compared to most mafic igneous units of the Kaapvaal craton. Fig. 14 presents the Th/Nb ratio of most of the mafic units in the craton from the 3.07 Ga Dominion Group to the 0.179 Ga Karoo LIP. Most of the mafic units of the Transvaal Supergroup show low Th/Nb ratios, except the low-Ti Umkondo magma, the B1 units of the Rustenburg Layer Suite (Bushveld Complex) and the mafic igneous units in the first part of the Paleoproterozoic, which include the Hekpoort and Ongeluk formations. In other words, the ~2.43 Ga Ongeluk Formation and the associated ~2.44 Ga Westerberg Sill (*Gumsley et al., 2017*), the ~2.3 Ga Bushy Bend lava, the ~2.23 Ga Hekpoort Formation and the ~2.21 Ga Mashishing dyke swarm (*Wabo et al., in press*) show high Th/Nb ratios which contrast sharply with units older than the Ongeluk Formation. To emphasise the offset of Th/Nb around the Archean – Proterozoic boundary, this ratio has respectively a mean of 0.31 ± 0.18 with $0.05 < Th/Nb < 0.88$ in the Archean (based on 164 samples) and a mean of 1.21 ± 0.26 with $0.80 < Th/Nb < 1.90$ in the Paleoproterozoic from the 2.44 Ga Westerberg Sills to the 2.21 Ga Mashishing dyke swarm (based on 76 samples).

In summary, the data presented here indicate that the SCLM below the Kaapvaal craton changed close to the Archean - Proterozoic transition, and remained stable for at least 200 Myr.

Three scenarios could explain such a change: (1) plume-related mafic underplating at the crust-mantle boundary, (2) subduction imbrication of Archean oceanic lithosphere in the root of the Kaapvaal Craton, and (3) metasomatic enrichment of the mantle wedge as a result of subduction of enriched, likely crustal, material. The above possibilities were already mentioned by *Zirakparvar et al. (2014)* to explain the origin of the Bushveld parent magmas. According, *Zirakparvar et al*., the Hf isotope data of the Bushveld Complex are consistent with generation of the Bushveld parent magmas by partial melting in a SCLM source which began to evolve in isolation from the depleted mantle around 2.6 Ga, which they explain by the three scenarios mentioned. The source(s) of the lavas of the Hekpoort and Ongeluk formations and those of the Bushveld Complex could potentially be related, explaining the high Th/Nb ratio of the B1 units of the Rustenburg Layered Suite (Fig. 14). However, the lack of Hf isotope data for either the Hekpoort or Ongeluk formations prevents us to test this hypothesis. By focusing on the data presented here, the high Th/Yb (Fig. 12), Th/Nb (Fig. 14) and moderate Nb/Yb (Fig. 12) ratios of both the Hekpoort and Ongeluk formations suggest preferential enrichment in Th which is in disagreement with plume related magmatism (as discussed in section 6.3). Thus, the geochemical data for both the Hekpoort and Ongeluk formations show that an important subduction event marked the Archean-Proterozoic boundary in the Kaapvaal craton.

A change in magmatism during this transition was already described by *Srivastava (2008)* and *Srivastava and Ernst (2013)*. These authors noted that the end of widespread komatiite magmatism at the end of the Neoarchean is associated with the onset of a period of BN magmatism globally, which became rare after 2 Ga. According these authors, boninitic magmatism is a reflection of a three-step process: (1) Extraction of mafic magma forming the widespread Archean greenstone belts and developing a complementary refractory mantle, which becomes the lithospheric root of the cratons; (2) Crustal thickening at the end of Archean, i.e., the assembly of several Archean cratons at ca. 2.7 Ga. The SCLM of the cratons, which started out refractory would have been metasomatised during this assembly; (3) Partial melting of this metasomatised mantle producing BN-type melts, either as a result of the arrival of mantle plumes or associated with the breakup of Late-Archean continents. The Hekpoort/Ongeluk formation lavas follow this model to some extent. However, for *Srivastava (2008)* and *Srivastava and Ernst (2013)* the second step also corresponds to cratonization, which is not the case for the Kaapvaal craton which became stable before 3 Ga and not at the end of the Archean (e.g., *de Wit et al., 1992*; *Eriksson et al., 2002*; *Schoene et al., 2009*). Since ca. 3.1 Ga, several basins and sub-basins developed on the Kaapvaal craton, with quasi-continuous sedimentation until ~ 1.8 Ga, interrupted by several volcanic episodes (Fig. 14).

Finally, for the Kaapvaal craton, the evolution from mafic igneous events with low Th/Nb ratios to high Th/Nb ratios as presented in figure 14 is likely related to geodynamic changes during or close to the Archean-Proterozoic boundary that were either local or worldwide, but these changes were unrelated to cratonization.

Conclusions

New field observations (including vesicle cylinders, hyaloclastites, variolitic lavas, and the presence of crustal xenoliths) in the Hekpoort lava show that volcanoclastic rocks actually represent a small portion of the Hekpoort Formation and area, stratigraphically located at the base. Irrespective of the structures and location, the lavas are characterized by trace element patterns, which are indistinguishable from the patterns of the 200 myr older Ongeluk lavas in the Griqualand West sub-basin. More importantly, the close geochemical similarity between two different mafic igneous units of the Kaapvaal craton remains so far an isolated case across the Kaapvaal craton stratigraphy, which encompasses mafic igneous provinces of ca. 3.0 Ga to the Phanerozoic. This, together with the relatively high content of both U and Th in the two formations, suggest that their sources of the primary magma were similar, and may point towards a change in composition of the Kaapvaal SCLM around the Archean – Proterozoic boundary, this change being possibly related to subduction processes.

Acknowledgements:

We would like to thank Richard Ernst and two anonymous reviewers, as well as the editor, Randall Parrish, whose comments and suggestions have improved the manuscript considerably. We also want to thank Jérémie Lehmann for his help regarding figure 11. Funding was provided by grants from South African Department of Science and Technology and the National Research Foundation (DST-NRF)–funded Centre of Excellence for Integrated Mineral and Energy Resource Analysis (CIMERA). Funding to Wladyslaw Altermann for fieldwork by the team of the University of Pretoria (UP) was from the NRF incentive funding for rated researchers and by the Kumba-Exxaro Chair at UP.

References:

Altermann, W., Hälbich, I.W. 1991. Structural history of the south-western corner of the Kaapvaal craton and the adjacent Namaqua realm: New observations and reappraisal. Precambrian Research 52, 133-166.

Altermann, W., Lenhardt, N. 2012. The volcano-sedimentary succession of the Archean Sodium Group, Ventersdorp Supergroup, South Africa: Volcanology, sedimentology and geochemistry. Precambrian Research 214-215, 60-81.

Altermann, W., van Kranendonk, M. J., Humbert, F., Cornell, D. H. (Submitted). The end of the Early Proterozoic glaciation and the Ongeluk – Hekpoort Large Igneous Province of the Kaapvaal Craton, South Africa. 27th Colloquium of African Geology, Abstract Volume, Aveiro, Portugal, July 2018.

Armstrong, N.V., Wilson, A.H., hunter, D.R. 1986. The Nsuze Group, Pongola Sequence, South Africa: Geochemical evidence for Archean volcanism in a continental setting. Precambrian Research 34, 175 – 203.

Arndt, N.T., Czamanske, G.K., Wooden, J.L., Fedorenko, V.A. 1993. Mantle and crustal contributions to continental flood volcanism. Tectonophysics 223, 39–52.

Arndt, N.T., Fleet, M.E. 1979. Stable and metastable pyroxene crystallization in tayered komatiite lava flows. American Mineralogist 64, 856-864.

Barnes, S.-J., Maier, W.D., Curl, E.A. 2010. Composition of the marginal rocks and sills of the Rustenburg Layered Suite, Bushveld Complex, South Africa: Implications for the formation of the platinum-group element deposits. Economic Geology 105, 1491-1511.

Bau, M., Romer, R.L., Lüders, V., Beukes, N.J. 1999. Pb, O, and C isotopes in silicified Mooidraai dolomite (Transvaal Supergroup, South Africa): implications for the composition of Paleoproterozoic seawater and 'dating' the increase of oxygen in the Precambrian atmosphere. Earth Planetary Science Letters 174, 43–57.

Bengtson, S., Rasmussen, B., Ivarsson, M., Muhling, J., Broman, C., Marone, F., Stampanoni, M., Bekker, A. 2017. Fungus-like mycelial fossils in 2.4-billion-year-old vesicular basalt. Nat. Ecol. Evol. 1, 0141. DOI: 10.1038/s41559-017-0141

Beukes, N.J., Dorland, H., Gutzmer, J., Nedachi, M., Ohmoto, H. 2002. Tropical laterites, life on land, and the history of atmospheric oxygen in the Paleoproterozoic. Geology 30, 491–494.

Beukes N.J., Frei D., Vorster C. 2013. Detrital zircon age constraints of the Makganyene Snowball Earth Event (South Africa) at 2.25-2.22 Ga: the youngest of four Huronian glaciations? In: Geological Societry of America Abstracts with Programs, Denver, Colorado USA, 2013. vol 7. p 340.

Bowen, T.B., Marsh, J.S., Bowen, M.P., Eales, H.V. 1986. Volcanic rocks of the Witwatersrand triad, south Africa. I: Description, classification and geochemical stratigraphy. Precambrian Research 31, 297-324.

Buchanan, P.C., Koeberl, C., Reimold, W.U. 1999. Petrogenesis of the Dullstroom Formation, Bushveld Magmatic Province, South Africa. Contrib. Mineral. Petrol. 137, 133-146.

Burger, A.J., Coertze, F.J. 1973. Radiometric age determinations on rocks from southern Africa up to the end of 1971.Bulletin Geological Society South Africa 58, 1-46.

Burke, K., Gunnell, Y. 2008. The African Erosion Surface: A Continental-Scale Synthesis of Geomorphology, Tectonics, and Environmental Change over the Past 180 Million Years. Geol. Soc. Am. Memoir 201, 66pp.

Busby, C.J., Garrison, N., Gans, P., Wagner, D. 2004. Mid-Miocene tholeiitic basalt in the ancestral Cascades arc: geology, volcanology and geochronology of the Lovejoy Basalt. Geol. Soc. Am., Abstracts with Programs 36, 97.

Button, A. 1973. A regional study of the stratigraphy and development of the Transvaal Basin in the eastern and north-eastern Transvaal. Ph.D. thesis, University of Witwatersrand, Johannesburg, 352 pp.

Button, A. 1974. Low potash pillow basalts in the Pretoria Group, Transvaal Supergroup. Trans. Geol. Soc. S. Africa 77, 99-104.

Button, A. 1986. The Transvaal sub-basin of the Transvaal sequence. - In: Anhaeusser, C.R. & Maske, S., (eds.). Mineral deposits of Southern Africa. - Geol Soc. S. Afr., Johannesburg, 811-817.Cheney, E.S. 1996. Sequence stratigraphy and plate tectonic significance of the Transvaal succession of Southern Africa and its equivalent in Western Australia. Precambrian Research 79, 3-24.

Coetzee, L.L. 2001. Genetic stratigraphy of the Paleoproterozoic Pretoria Group in the Western Transvaal. M.Sc. thesis, Rand Afrikaans University.

Cole, P.D., Calder, E.S., Sparks, R.S.J., Clarke, A.B., Druitt, T.H., Young, S.R., Herd, R.A., Harford, C.L., Norton, G.E. 2002. Deposits from dome-collapse and fountaincollapse pyroclastic flows at Soufrière Hills Volcano, Montserrat. In: Druitt, T.H., Kokelaar, B.P. (Eds.), The Eruption of Soufrière Hills Volcano, Montserrat, from 1995 to 1999. Geol. Soc. Lond., Mem. 21, 231–262.

Cornell, D.H., Schütte, S.S., Eglington, B.L. 1996. The Ongeluk basaltic andesite formation in Griqualand West, South Africa: submarine alteration in a 2222 Ma Proterozoic sea. Precambrian Research 79, 101–123.

Cox, P.A. 1995. The Elements on the Earth. Oxford Univ. Press, 287 pp.

Cox, K.G., Bell, J.D., Pankhurst, R.J. 1979. The Interpretation of Igneous Rocks. George Allen and Unwin, London, 450 pp.

Crow, C., Condie, K.C. 1987. Geochemistry and origin of late Archean volcanics from the Rhenosterhock Formation, Dominion Group, South Africa. Precambrian Research 37, 217-229.

Crow, C., Condie, K.C. 1990. Geochemistry and origin of early Proterozoic volcanic rocks from the Transvaal and Soutpansberg successions, South Africa. Precambrian Research 47, 17–26.

Davidson, J., Turner, S., Handley, H., Macpherson, C., Dosseto, A., 2007. Amphibole "sponge" in arc crust? Geology, 35, 787-790.

Deegan, F M., Troll, V.R., Freda, C., Misiti, V., Chadwick, J.P., McLeod, C.L., Davidson, J.P. 2010. Magma–carbonate interaction processes and associated CO2 release at Merapi Volcano, Indonesia: insights from experimental petrology. Journal of petrology 51, 1027-1051.

DePaolo, D.J. 1988. Neodymium Isotope Geochemistry. An Introduction. in Wyllie, P.J., Minerals and Rocks Series 20. Springer-Verlag, 187pp.

Dorland, H.C., 2004. Provenance Ages and Timing of Sedimentation of Selected Neoarchean and Paleoproterozoic Successions on the Kaapvaal craton. Unpublished Ph.D. thesis, Rand Afrikaans University, Johannesburg, South Africa, 326 pp.

de Wit, M.J., Roering, C., Hart, R.J., Armstrong, R.A., de Ronde, C.E.J., Green, R.W.E., Tredoux, M., Peberdy, E. and Hart, R.A., 1992. Formation of an Archaean continent, Nature 357, 553-562.

de Wit, M.C.J., Ward, I.D., Bamford M.K., Roberts, M.J. 2009. The significance of the Cretaceous diamondiferous gravel deposit at Mahura Muthla, Northern Cape Province, South Africa. South African Journal of Geology 112, 89-108.

du Toit, A.L., 1926. The Geology of South Africa, Oliver & Boyd, London, 444pp.

Elburg, M., 2010. Sources and processes in arc magmatism: the crucial role of water. Geologica Belgica 13, 121–135.

Elburg, M., Goldberg, A., 2000. Age and geochemistry of Karoo dolerite dykes from northeast Botswana. Journal of African Earth Sciences 31, 539-554.

Engelbrecht, J.P., 1986. Die Bosveld Kompleks en sy vloergesteentes in die omgewing van Nietverdiend, Wes-Transvaal. Ph.D. thesis, University of Pretoria.

Eriksson, P.G., Altermann, W., 2013. Paleoproterozoic glacial deposits of South Africa (Chapter 7.2.2). In: Melezhik, V.A., Kump, L.R., Fallick, A.E., Strauss, H., Hanski, E.J., Prave, A., Lepland, A. (Eds.), Reading the Archve of Earth's Oxygenation, Global Events and the Fennoscandian Arctic Russia- Drilling Early Earth Project, vol. 3. Springer, Berlin, pp. 1083-1096.

Eriksson, P.G., Altermann, W., Hartzer, F.J., 2006. The Transvaal Supergroup and its precursors. In: Johnson, M.R., Anhaeusser, C.R., Thomas, R.J. (Eds.), The Geology of South Africa. Geol. Soc. S. Afr., Council for Geoscience, Pretoria, Johannesburg, 237–260.

Eriksson, P.G., Altermann, W., Hartzer, F.J. 2006. The Transvaal Supergroup and Precursors. Chapter 10 In: Johnson, MR., Annhaeusser, CR. Thomas, RJ. (Editors): The Geology of South Africa. Geol. Society of South Africa. 237-260.

Eriksson, P.G. Cheney, E.S. 1992. Evidence for the transition to an oxygen-rich atmosphere during the evolution of red beds in the Lower Proterozoic sequences of southern Africa. Precambrian Research 54, 257-269.

Eriksson, P.G., Condie, K.C., van der Westhuizen, W., van der Merwe, R., de Bruiyn, H., Nelson, D.R., Altermann, W., Catuneanu, O., Bumby, A.J., Lindsay, J., CunninghamM.J. 2002. Late Archaean superplume events: a Kaapvaal-Pilbara perspective. J. Geodynamics 34, 207-247.

Eriksson, P.G., Hattingh, P.J., Altermann, W. 1995. An overview of the geology of the Transvaal Sequence and the Bushveld Complex, South Africa. - Mineralium Deposita, 30/2, 98-111

Eriksson, P.G., Reczko, B.F.F. 1995. The sedimentary and tectonic setting of the Transvaal Supergroup floor rocks to the Bushveld Complex: tectonic setting derived from basin-fill geometry, inferred volcanic processes and sedimentation systems. J. Afr. Earth Sci. 21, 487–504.

Eriksson, P.G., Twist, D. 1986. A note on a lahar deposit in the Hekpoort Formation, Transvaal Sequence, near Pretoria. Trans. Geol. Soc. S. Afr. 89, 415–418.

Ernst, R.E. (2014). Large Igneous Provinces. Cambridge University Press 653 p.

Evans, D.A.D., Beukes, N.J., Kirschvink, J.L. 1997. Low-latitude glaciation in the Palaeoproterozoic era. Nature, 386, 262–266.

Fairey, B., Tsikos, H., Corfu, F., Polteau, S. 2013. U–Pb systematics in carbonates of the Postmasburg Group, Transvaal Supergroup, South Africa: primary versus metasomatic controls. Precambrian Research 231, 194–205.

Fisher, R.V., Schmincke, H.U. 1984. Pyroclastic Rocks. Springer, Berlin.

Gardner, J.E., Befus, K.S., Miller, N.R., Monecke, T. 2014. Cooling rates of mid-ocean ridge lava deduced from clinopyroxene spherulites. Journal of Volcanology and Geothermal Research 282, 1–8.

Godinot, A. 1988. Comment on ‘Pipe vesicles in Hawaiian basaltic lavas: their origin and potential as paleoslope indicators’. Geology 16, 90.

Gomwe, T.E.S. 2006: A geochemical profile through the Uitkomst Complex on the farm Slaaihoek, with special reference to the platinum – group elements and Sm–Nd isotopes. B.Sc. thesis. University of Natal, Durban, South Africa. 107 pp.

Grant, C.E. 2003. The physical volcanology and geochemistry of the Nsuze Group, Pongola Supergroup, of northern KwaZulu-Natal and southeastern Mpumalanga. M.Sc. thesis. University of Pretoria, 219 pp.

Green, T.H., Ringwood, A.E. 1968. Crystallization of basalt and andesite under high pressure hydrous conditions. Earth Planetary Science Letters 3, 481-489.

Grobler, N.J., Botha, B.J.V. 1976. Pillow lavas and hyaloclastites in the Ongeluk andesite formation in a road-cut west of Griquatown, South Africa. Trans. Geol. Soc. S. Afr. 79, 53–57.

Gumsley, A.P., Chamberlain, K., Bleeker, W., Söderlund, U., de Kock, M.O., Larsson, E., Bekker, A. 2017. The timing and tempo of the Great Oxidation Event. Proc. Natl. Acad. Sci. USA, 114, 1811-1816. doi:10.1073/pnas.1608824114.

Gutzmer, J., Banks, D.A., Lüders, V., Hoefs, J., Beukes, N.J., von Bezing, K.L. 2003. Ancient sub-seafloor alteration of basaltic andesites of the Ongeluk Formation, South Africa: implications for the chemistry of Paleoproterozoic seawater. Chem. Geol. 201, 37–53.

Harmer, R.E., von Gruenewaldt, G. 1991. A review of magmatism associated with the Transvaal Basin. - implications for its tectonic setting. S. Afr. J. Geol. 94, 104-122.

Hanson, R.E., Gose, W.A., Crowley, J., Ramezani, S.A., Bowring, D.S., Hall, R.P., Pancake, J.A., Mukwakwami, J. 2004. Paleoproterozoic intra-plate magmatism and basin development on the Kaapvaal craton: age, paleomagnetism and geochemistry of ~1.93 to ~1.87 Ga post-Waterberg dolerites. South African Journal of Geology 107, 233-254.

Henkel, H., Reimold, W.U. 1998. Integrated geophysical modelling of a giant, complex impact structure: anatomy of the Vredefort Structure, South Africa. Tectonophysics, 287, 1–20.

Hoffman, P.F. 2013. The Great Oxidation and a Siderian snowball Earth: MIF-S based correlation of Paleoproterozoic glacial epochs. Chem. Geol., 362, 143–156.

Holland, H.D., Beukes, N.J. 1990. A paleoweathering profile from Griqualand West, South Africa: evidence for a dramatic rise in atmospheric oxygen between 2.2 and 1.9 by bp. Am. J. Sci., 290, 1-34.

Holland, H.D., Rye, R., Ohmoto, H. 1997. Evidence in pre-2.2 Ga paleosols for the early evolution of atmospheric oxygen and terrestrial biota–discussion and reply. Geology 25, 857–858.

Humbert, F., de Kock, M., Altermann, W., Lenhardt, N. (in revision b). Neoarchean to early Paleoproterozoic within-plate volcanism of the Kaapvaal Craton: comparing the Ventersdorp Supergroup and the Ongeluk and Hekpoort formations (Transvaal Supergroup). Springer special volume

Humbert., F., Elburg, M., Ossa Ossa, F., de Kock, M., Robion, P. (in revision a). Variolites of the Paleoproterozoic Hekpoort Formation (Transvaal sub-basin, Kaapvaal craton): multistage undercooling textures? Lithos

Humbert, F., Sonnette, L., de Kock, M.O., Robion, P., Horng, C.S, Cousture, A., Wabo, H. 2017. Palaeomagnetism of the early Palaeoproterozoic, volcanic Hekpoort Formation (Transvaal Supergroup) of the Kaapvaal craton, South Africa. Geophys. J. Int. 209, 842–865. DOI: 10.1093/gji/ggx055

Jerram, D.A., 2002. Volcanology and facies architecture of flood basalts. In: Menzies, M.A., Klemperer, S.L., Ebinger, C.J., Baker, J. (eds) Volcanic Rifted Margins. Geological Society of America Special Paper 362, 121-135.

Jourdan, F., Bertrand, H., Scharer, U., Blichert-Toft, J., Feraud, G., Kampunzu, A.B. 2007. Major and trace elements and Sr, Nd, Hf, and Pb isotope compositions of the Karoo Large Igneous Province, Botswana-Zimbabwe: Lithosphere vs Mantle plume contribution. Journal of Petrology 48, 1043-1077.

Kamo, S.L., Reimold, W.U., Krogh, T.E., Colliston, W.P. 1996. A 2.023 Ga age for the Vredefort impact event and a first report of shock metamorphosed zircons in pseudotachylitic breccias and Granophyre. Earth Planet. Sci. Lett., 144, 369–387.

Kaźmierczak, J., Kremer, B., Altermann, W., Franchi, I. 2016. Tubular microfossils from 2.8 to 2.7 Ga-old lacustrine deposits of South Africa: A sign for early origin of eukaryotes? Precambrian Res. 286, 180-194.

Klausen, M. B., Söderlund, U., Olsson, J. R., Ernst, R.E., Armoogam, M., Mkhize, S.W., Petzer, G.,2010. Petrological discrimination among Precambrian dyke swarms: Eastern Kaapvaal craton (South Africa). Precambrian Research 183, 501-522.

Kobayashi, T., Ishihara, K., Suzuki-Kamata, K., Fukushima, D. 2003. Sakurajima volcano and pyroclastic deposits in southern Kyushu, IUGG 2003 Field Trip Guidebook. Volcanol. Soc. Jpn., 105–131.

Lenhardt, N., Eriksson, P.G., Catuneanu, O., Bumby, A.J. 2012. Nature of and controls on volcanism in the ca. 2.32-2.06 Ga Pretoria Group, Transvaal Supergroup, Kaapvaal craton, South Africa. Precambrian Research 214-215, 106-123.

Letts, S., Torsvik, T.H., Webb, S.J., Ashwal, L.D. 2009. Palaeomagnetism of the 2054 Ma Bushveld Complex (South Africa): implications for emplacement and cooling. Geophys. J. Int., 179, 850–872.

Lindsley, D.H. 1983. Pyroxene thermometry. American Mineralogist 68, 477-493.

McPhie, J., Doyle, M., Allen, R. 1993. Volcanic Textures: A guide to the interpretation of textures in volcanic rocks. University of Tasmania. Centre for Ore Deposit and Exploration Studies, 198 pp.

Maier, W., Arndt, N., Curl, E. 2000. Progressive crustal contamination of the Bushveld Complex: evidence from Nd isotopic analyses of the cumulate rocks. Contrib. Mineral Petrol 140, 316–327.

Marsh, J.S., Bowen, M.P., Rogers, N.W., Bowen, T.B. 1989. Volcanic rocks of the Witwatersrand Triad, South Africa. II: Petrogenesis of mafic and felsic rocks of the Dominion Group. Precambrian Research 44, 39-65.

Marsh, J.S., Bowen, M.P., Rogers, N.W., Bowen, T.B. 1992. Petrogenesis of late Archean flood-type basic lavas from the Klipriviersberg Group, Ventersdorp Supergroup, South Africa. J. Petrol. 33, 817–847.

Miyabuchi, Y., Watanabe, K., Egawa, Y. 2006. Bomb-rich basaltic pyroclastic flow deposit from Nakadake, Aso Volcano, southwestern Japan. J. Volcanol. Geotherm. Res. 155, 90–103.

Moore J.M., Polteau, S., Armstrong, R.A., Corfu, F., Tsikos, H. 2012. The age and correlation of the Postmasburg Group, southern Africa: Constraints from detrital zircon grains. J. Afr. Earth Sci. 64, 9–19.

Moore, J.M., Tsikos, H., Polteau, S. 2001. Deconstructing the Transvaal Supergroup, South Africa: implications for Palaeoproterozoic palaeoclimate models. J. Afr. Earth Sci. 33, 437–444.

Mukasa, S.B., Wilson, A.H., Young, K.R. 2013. Geochronological constraints on the magmatic and tectonic development of the Pongola Supergroup (Central Region), South Africa. Precambrian Research 224, 268–286.

Myers, R.E., Cawthorn, R.G., McCarthy, T.S., Anhaeusser, C.R., 1987. Fundamental uniformity in the trace element patterns of the volcanics of the Kaapvaal craton from 3000 to 2100 Ma: evidence for the lithospheric origin of these continental tholeiites. Geol. Soc. S. Afr., Spec. Publ. 33, 315–326.

Nelson, D.R., Trendall, A.F., Altermann, W. 1999. Chronological correlations between the Pilbara and Kaapvaal cratons. Precambrian Research 97, 165-189.

Nelson, D.R., Trendall, A.F., de Laeter, J.R., Grobler, N.J., Fletcher, I.R., 1992. A comparative studies of the geochemical and isotopic systematics of late Archean flood basalts from the Pilbara and Kaapvaal cratons. Precambrian Research 54, 231–256.

Nesbitt, H.W., Young, G.M. 1982. Early Proterozoic climates and plate motions inferred from major element chemistry of lutites. Nature 299, 715–717.

Oberholzer, J.D. 1995. Die geologie van die piroklastiese gesteentes in die Hekpoort Formasie, Transvaal Opeenvolging. MSc. thesis, University of Pretoria.

Oberholzer, J.D., Eriksson, P.G. 2000. Subaerial volcanism in the Palaeoproterozoic Hekpoort Formation (Transvaal Supergroup), Kaapvaal craton. Precambr. Res. 101, 193–210.

Ohmoto, H. 1996. Evidence in pre-2.2 Ga paleosols for the early evolution of atmospheric oxygen and terrestrial biota. Geology 24, 1135–1138.

Ohmoto, H. 2004. Archean Atmosphere, Hydrosphere and Biosphere. In: Eriksson, P.G., Altermann, W., Nelson, D.R., Mueller, W., Catuneanu, O. (Eds.) 2004: The Precambrian Earth: Tempos and Events; Elsevier: “Developments in Precambrian Geology 12, 361-388.

Olsson, J.R., Klausen, M.B., Hamilton, M.A., März, N., Söderlund, U., Roberts, R.J. 2016. Baddeleyite U-Pb ages and geochemistry of the 1875 -1835 Ma Black Hills Dyke Swarm across north-eastern South Africa: Part of a trans-Kalahari Craton back-arc setting? GFF 00, 1-20. doi:http://dx.doi.org/10.1080/11035897.2015.1103781.

Palme, H., O'Neill, H.St.C. 2004. Cosmochemical estimates of Mantle Composition. In: Treatise on Geochemistry. Holland, H.D. and Turrekian, K.K. (Editors), Elsevier, Amsterdam, The Netherlands 2, 1-38.

Partridge T.C., Maud R.R. 2000. The Cenozoic of Southern Africa, Oxford monograph no. 40. Oxford University Press, New York, 406 pp.

Pearce, J.A. 1996. A user's guide to basalt discrimination diagrams. In D.A. Wyman (eds.): Trace Element Geochemistry of Volcanic Rocks: Applications for Massive Sulphide Exploration, Geological Association of Canada, Short Course Notes 12, 79-133.

Pearce, J.A. 2008. Geochemical fingerprinting of oceanic basalts with applications to ophiolite classification and the search for Archean oceanic crust. Lithos 100, 14–48.

Pearce, J.A., Robinson, P.T., 2010. The Troodos ophiolitic complex probably formed in a subduction initiation, slab edge setting. Gondwana Research, 18: 60–81.

Philpotts, A., Lewis, C. 1987. Pipe vesicles – an alternative model for their origin. Geology 15, 971–974.

Rajesh, H.M., Chisonga, B.C., Shindo, K., Beukes, N.J., Armstrong, R.A., 2013. Petrographic, geochemical and SHRIMP U-Pb titanite age characterization of the Thabazimbi mafic sills: Extended time frame and a unifying petrogenetic model for the Bushveld Large Igneous Province. Precambrian Research 230, 79-102.

Reczko, B.F.F., Oberholzer, J.D., Res, M., Eriksson, P.G., Schreiber, U.M., 1995. A revaluation of the volcanism of the Palaeoproterozoic Pretoria Group (Kaapvaal craton) and a hypothesis on basin development. Journal Africa Earth Science 21, 505–519.

Retallack, G.J., Krinsley, D.H. 1993. Metamorphic alteration of a Precambrian (2.2 Ga) paleosol from South Africa. Precambrian Research 63, 27–41.

Retallack, G.J., Krull, E.S., Thackray, G.D., Parkinson, D. 2013. Problematic urn-shaped fossils from a Paleoproterozoic (2.2 Ga) paleosol in South Africa. Precambrian Res. 235, 71-87.

Rollinson, H., 1993. Using Geochemical Data: Evolution, Presentation, Interpretation. Longman Scientific & Technical, 352p.

Rudnick, R.L., Fountain, D.M. 1995. Nature and composition of the continental crust—a lower crustal perspective. Rev. Geophys. 33, 267–309.

Santos Barreto, C.J., Fernandes de Lima, E., Scherer, C.M., May Rossetti L. de M. 2014. Lithofacies analysis of basic lava flows of the Paraná igneous province in the south hinge of Torres Syncline, Southern Brazil, Journal of Volcanology and Geothermal Research 285, 81-99.

Saucedo, R., Macías, J.L., Bursik, M., Mora, J.C., Gavilanes, J.C., Cortes, A. 2002. Emplacement of pyroclastic flows during the 1998–1999 eruption of Volcán de Colima, Mexico. J. Volcanol. Geotherm. Res. 117, 129–153.

Schreiber, U.M. 1991. A palaeoenvironmental study of the Pretoria Group in the eastern Transvaal. Ph.D. thesis, University of Pretoria.

Schröder, S., Beukes, N.J., Armstrong, R.A. 2016. Detrital zircon constraints on the tectonostratigraphy of the Paleoproterozoic Pretoria Group, South Africa. Precambrian Research, 278, 362–393.

Schütte, S.S., 1992. Ongeluk volcanism in relation to the Kalahari manganese deposits. Unpubl. Ph.D. thesis, University of Natal, 255 pp.

Sharpe, M.R., Brits, R., Engelbrecht, J.P., 1983. Rare earth and trace element evidence pertaining to the petrogenesis of 2.3 Ga old continental andesites and other volcanic rocks from the Transvaal Sequence, South Africa. University of Pretoria Institute for Geological Research on the Bushveld Complex Research Report 40, 63 pp.

Shellnutt, J.G., Zellmer, G.F. 2010. High-Mg andesite genesis by upper crustal differentiation. Journal of the Geological Society London 167, 1081–1088. doi: 10.1144/0016-76492010-070.

Schoene, B., Dudas, F.O.L., Bowring, S.A. and de Wit, M., 2009. Sm–Nd isotopic mapping of lithospheric growth and stabilization in the eastern Kaapvaal craton. Terra Nova 21, 219–228. doi: 10.1111/j.1365-3121.2009.00877.x

Shibuya, T., Komiya, T., Takai, K., Maruyama, S., Russell, M.J. 2017. Weak hydrothermal carbonation of the Ongeluk volcanics: evidence for low CO2 concentrations in seawater and atmosphere during the Paleoproterozoic global glaciation. Progress in Earth and Planetary Science, 4:31. DOI 10.1186/s40645-017-0145-6.

Shields, J.K., Mader, H.M., Caricchi, L., Tuffen, H., Mueller, S., Pistone, M., Baumgartner, L. 2016. Unravelling textural heterogeneity in obsidian: Shear-induced outgassing in the Rocche Rosse flow. Journal of Volcanology and Geothermal Research 310, 137-158. DOI:10.1016/j.jvolgeores.2015.12.003Sun, S.-s., McDonough,W.F., 1989. Chemical and isotopic systematics of oceanic basalts: implications for mantle composition and processes. Geol. Soc. Lond. Spec. Publ. 42, 313–345.

Smithies, R.H. 2002. Archaean boninite-like rocks in an intracratonic setting. Earth and Planetary Science Letters 197, 19-34.

Srivastava, R.K., 2008. Global intracratonic boninite-norite magmatism during the NeoArchean-Paleoproterozoic: evidence from the central Indian Bastar Craton. International Geology Review 50, 61–74.

Srivastava, R.K. & Ernst, R.E. (2013). Global intracratonic boninitic–norite magmatism during the Neoarchean–Paleoproterozoic: revisited. LIP of the Month, July 2013. See http://www.largeigneousprovinces.org/13jul.

Tatsumi, Y., Ishizaka, K. 1982. Origin of high-magnesian andesites in the Setouchi volcanic belt, southwest Japan, I. Petrographical and chemical characteristics. Earth and Planetary Science Letters 60, 293–304.

Van der Westhuizen, W.A., De Bruiyn, H., Meintjies, P.G., 2006. The Ventersdorp Supergroup, In: Johnson, M. R. and Anhaeusser, C. (Johnson, M. R. and Anhaeusser, C. (Eds.), The Geology of South Africa. Geological Society of South Africa/Council for Geoscience, Johannesburg/Pretoria, 187-208.

Van Kranendonk, M.J. with contributions by: W. Altermann, B.L. Beard, P.F. Hoffman, C.M. Johnson, J.F. Kasting, V.A. Melezhik, A.P. Nutman, D. Papineau and F. Pirajno. 2012. A chronostratigraphic division of the Precambrian: Possibilities and challenges. In: Gradstein, F.M., Ogg, J., Schmitz, M., Ogg, G. (Edits.): Geologic Time Scale 2012. IUGS Special Publ. Elsevier, 299-392.

Wabo, H., Humbert, F., de Kock, M.O., Belyanin, G., Söderlund, U., Maré, L.P., Beukes, N.J. in submission to Precambrian Research. Constraining the chronology of Mashishing dykes in the Mpumalanga Province: Identification of a new pre-Bushveld (~2.20 Ga) dyke swarm in the Kaapvaal craton (South Africa).

Wiggering, H., Beukes, N.J. 1990. Petrography and geochemistry of a 2000-2200 Ma-old hematitic paleo-alteration on Ongeluk basalt of the Transvaal Supergroup, Griqualand West, South Africa. Precambrian Research 46, 241-258.

Wilmoth, R.A., Walker, G.P. 1993. P-type and S-type pahoehoe: a study of vesicle distribution patterns in Hawaiian lava flows. J. Volcanol. Geotherm. Res. 55, 129–142.

Winchester, J.A., Floyd, P.A., 1977. Geochemical discrimination of different magma series and their differentiation products using immobile elements. Chem. Geol. 20, 325–343.

Wood, B.J., Turner, S.P. 2009. Origin of primitive high-Mg andesite: Constraints from natural examples and experiments. Earth and Planetary Science Letters 283, 59–66.

Worrall, F., Pearson, D.G. 2001. Water–rock interaction in an acidic mine discharge as indicated by rare earth element patterns. Geochim. Cosmochim. Acta 65, 3027–3040.

Yang, W., Holland H.D., 2003. The Hekpoort paleosol profile in Strata 1 at Gaborone, Botswana: soil formation during the Great Oxidation Event. Am. J. Sci., 303, 187–220.

Zeh, A., Ovtcharova, M., Wilson, A.H., Schaltegger, U., 2015. The Bushveld Complex was emplaced and cooled in less than one million years - results of zirconology, and geotectonic implications. Earth and Planetary Science Letters 418, 103-114.

Zirakparvar, N.A., Mathez, E.A., Scoates, J.S., Wall, C.J., 2014. Zircon Hf isotope evidence for an enriched mantle source for the Bushveld Igneous Complex. Contrib Mineral Petrol 168, 1050. DOI 10.1007/s00410-014-1050-2

Figure and table captions:

Figure 1: Distribution of the outcrops of the Bushveld Complex and the Transvaal Supergroup with emphasis on the Hekpoort lava formation in the Transvaal sub-basin (TB) and the Ongeluk lava formation in the Griqualand West sub-basin (GWB); compiled from 1:250000 South African geological maps. The location of the craton is specified in the upper right corner and the location of both basins within it is shown in the bottom right inset. The Kanye sub-basin is not represented. The Bushveld Complex indicated here includes the Rooiberg Group, the Rustenberg Layered Suite, the Rashoop Granophyre and the Lebowa Granite. The red rectangles and the red ellipse represent the studied areas; the rectangles emphasizing zones with outcrops (zones sampled: solid rectangles; the Hekpoort river valley: dashed rectangle). The dashed circle segment represents the maximum extension of the Vredefort Impact Structure according to *Henkel and Reimold (1998)*.

Figure 2: Chronostratigraphy of the Transvaal Supergroup based on *Gumsley et al. (2017)* and *Humbert et al. (2017*). The age dates are from: (1) *Moore et al. (2012)* - U-Pb on detrital zircon, (2) *Gumsley et al. (2017)* - U-Pb on baddeleyite, (3) *Bau et al. (1999)* – carbonate Pb–Pb isochron, (4) *Fairey et al. (2013)* - whole rock U-Pb isochron, (5) *Burger and Coertze (1973)* - whole rock Rb-Sr isochron, (6) *Cornell et al. (1996)* - whole rock Pb–Pb isochron, (7) *Schröder et al. (2016)* - U-Pb SHRIMP on detrital zircon, (8) *Dorland (2004)* - U-Pb SHRIMP on detrital zircon, (9) *Zeh et al. (2015)* - U-Pb on detrital zircon. The Kanye sub-basin stratigraphy is not represented. Das. = Daspoort; Dwa. = Dwaalheuwel; Str. = Strubenkop.

Figure 3: (a.) Composite vertical sections of the three main sampling zones. AC= amygdale layer rich in clinochlore: MTB = massive tuff-breccia; MLT = massive lapilli-tuff; PB =

pyroclastic breccias; PL = pahoehoe lava; PWTF = paleo-weathered flow top; SLT = stratified lapilli-tuff; VC = layer rich in vesicle cylinders. See text for discussion. (b.) N-S schematic cross-section of the Hekpoort Formation along the Hekpoort river valley.

Figure 4: (a.) Satellite image of the Potchefstroom syncline, with a close-up of the eastern side in (b.) showing an outlier of the Dwaalheuwel and Strubenkop formations above the Hekpoort Formation. Images are from the software Google Earth (images ©Digital Globe 2015). (c.) representative Hekpoort outcrops which in the most cases correspond to scattered lava boulders. (d.) lava sample, taken just below the unconformity between the Hekpoort Formation and Strubenkop Formation marked by an erosional surface, and showing enrichment in iron oxides. (e.) typical fresh sections of the Hekpoort lava rocks, with textures varying from aphanitic (sample DK) to hypocrystalline (sample PWD). Most of the samples show an intersertal texture (samples DTHB and GCEE). (f.) example of vesicle-rich flow top, being weathered (reddish parts) and with two fresh surfaces. (g.) example of volcanoclastic rocks (pyroclastic breccia), in which several angular clasts are visible.

Figure 5: (a.) and (b.) subparallel layers showing high concentrations of amygdales that can either be 'second order' lava flows or related to shear-induced outgassing; a tiny oblique vesicle cylinder can be also be seen in (b.). (c.) to (g.) vesicle cylinders in subvertical (c.) and subhorizontal (d., e., f.) sections with a fresh surface in (d.) and in thin section (g) showing the contact between the cylinder (left side) and the surrounding lava (right side). Some vesicle cylinders are asymmetrical (e.) or elongated (f.), likely linked to their development while the lava flow was still mobile. (h.) example of pahoehoe lava. (i.) to (l.) volcanoclastic rocks: stratified lapilli-tuff (i., j.) massive lapilli-tuff (k.), pyroclastic breccia showing a block that was a flow top (l.). Detail of limestone xenolith, showing rounded crystals of calcite in the massive

lapilli-tuff (m.). (n.) and (o.) interbedded sedimentary units in the area of Mooikloof of metamorphosed fine sandstone rich in iron oxide (o.). Some kink folding can be observed in the outcrop (n.) as well as in the thin section (o.). (p.) and (q.) hyaloclastites from the Potchefstroom syncline (Fig. 4) showing vesicle-rich block surrounded by breccias; see close-up in (p.). The up to half centimeter-thick yellow rim around (p.) is linked to recent weathering. (q.) evidence of palagonitisation. (r.) variolitic lava flows showing individual variolites and partly coalescent in the center of the picture. Diffusion areas between the variolites and the groundmass can be observed (bright 1-2 cm rims around the variolites). (s.) thin section of a small variolites. The center is occupied by an orthopyroxene crystal now fully pseudomorphosed by clinochlore.

Figure 6: (a.) to (c.) thin sections combining PPL and XPL modes, and (d.) to (f.) backscattered images. (a.) detail of a microlitic (hyalopilitic) texture. (b.) intersertal texture showing euhedral plagioclase, orthopyroxene (pseudomorphosed by clinochlore) and clinopyroxene. (c.) microlitic texture surrounding the plagioclase phenocrysts shown in Fig. 4c (sample PWD). Pseudomorphosed euhedral pyroxenes in between two vesicles (ves) filled by quartz (d.) and actinolite overgrowth on a preserved diopside (e.). (f.) interior of a variolite showing skeletal Cpx phenocrysts with a core pseudomorphosed by clinochlore in basal and longitudinal cross-section. The skeletal Cpx are surrounded by the acicular micrometric clinopyroxene composing the variolites. All Cpx are augite. Primary minerals: Aug = augite; Opx = orthopyroxene; Pl= plagioclase; Pgt = pigeonite; S-Pl = skeletal plagioclase. Secondary minerals (italic in the figures): Act = actinolite; Cal = calcite; Clc = clinochlore; Ep = epidote.

Figure 7: (a.) Ternary diagram presenting composition of clinopyroxenes (Cpx) in the Hekpoort lavas. Wo = wollastonite; En = enstatite; Fs = ferrosilite. The ‘augite core’ refers to

the biggest part of the augite, not only their center, while their ‘rim’ only correspond to the outer 10-20μm of the crystals. (b.) core augite and pigeonite data represented in a polythermal orthopyroxene - augite - pigeonite phases diagram showing 100°C intervals at P = 5kb (from *Lindsley, 1983*).

Figure 8: (a.) Classification diagram of *Winchester and Floyd (1977)*, modified by *Pearce (1996)* with the Hekpoort and Ongeluk samples. (b.) Same samples in the Total Alkali versus Silica (TAS; *Cox et al., 1979*). In the latter, the samples mainly plot in the range of basaltic andesite due to an increase of SiO_2 related to silicification and the pronounced scatter of samples along the Y axis is the consequence of K- and Na-metasomatism.

Figure 9: Variation diagrams displaying the content major oxides and some traces elements versus the Mg# for the same samples as in Fig. 8. The dotted correlation lines in some plots are only for the Hekpoort samples. The dotted areas include 95% of the Th and U data measured (by XRF) over 104 Ongeluk samples by *Schutte (1992)*. The Ongeluk sample showing the lowest SiO_2, Na_2O and highest K_2O contents correspond to the pillow rim.

Figure 10: REE (a, b) and multi-element diagrams (c, d) of the same samples as in Figs. 8 and 9. Samples were normalized to chondrites (REE diagram) and to primitive mantle (multi-element diagrams) respectively, after *Palme and O'Neill (2014)*. The shaded area behind the Ongeluk samples corresponds to the Hekpoort samples on the left.

Figure 11: Al_2O_3 versus Mg# for the Hekpoort and Ongeluk Formations compared to the values of (a) the Indonesian Arc (literature data from GeoRoc website http://georoc.mpchmainz.gwdg.de/georoc/ and own data), used here as an example subduction-

related magmas, and (b) the Karoo LIP lavas (GeoRoc and own data). Data are represented as density plots.

Figure 12: (a. to c.) Th/Yb versus Nb/Yb diagrams. Subduction zones have Nb/Yb ratios similar to Depleted Mantle, but higher Th/Yb ratios. Enriched mantle sources have higher Nb/Yb as well as Th/Yb ratios. The examples of crustal input model by contamination (b.) and subduction zone (SZ) component (c.) are taken from *Pearce (2008)*. In (b.), the AFC model is characterized by a rate of assimilation relative to the rate of crystallization r = 0.3; F = proportion of mass of magma remaining relatively to its initial mass. The SZC model in (c.) is based on $(Th/Nb)_{SZ}$ = 5 and $(Th_{SZ}/Th_{DM\text{-}magma})$ = 100; % = % SZ component in wedge. Note that the assimilation–fractional crystallization (AFC) and subduction zone component (SZC) models in Fig. 12(b, c) are from *Pearce (2008*) and purely indicative. DM = Depleted Mantle, PM = Primordial Mantle, EM = Enriched mantle, OIB = Oceanic Island Basalt source (*Sun and McDonough, 1989*), LC = Lower Crust, MC = Middle Crust, UC = Upper Crust, BC = Bulk Crust, PC = Phanerozoic Crust, AC = Archean Crust (*Rudnick and Fountain, 1995*).

Figure 13: REE diagrams comparing the Hekpoort pattern (black lines) presented in Fig. 10a with other mafic igneous units in the Kaapvaal craton from the Mesoarchean to the Phanerozoic; see Fig. 14 for references and ages of the units. RLS = Rustenburg Layer Suite; UM = ultramafic; n = number of samples plotted.

Figure 14: Th/Nb ratio of Neoarchean to Phanerozoic mafic units in the Kaapvaal craton. Sg = supergroup; n = number of samples plotted; a.a. = approximate age; Wester. S. = Westerberg Sills. Sg = supergroup; Do. = Dominion (group); Pon. = Pongola; Ven. = Ventersdorp; Wa. / So. = Waterberg and Soutspanberg (groups). The open circles represent the data and the black

squares the average value (calculated for units with more than 2 samples). The εNd(t) values were calculated for the age in the age column, * the εNd(t) of the Karoo LIP are quite inhomogeneous: 0.0 for the high-Ti dykes; -7.9 for the high-Ti picrites; -4.3 for the high-Ti lavas and sills and -2.1 for the low-Ti lavas.

Table 1: Location of examples of the specific features in the Hekpoort Formation. The star indicates very localized outcrops; other outcrops either correspond to a large area, notably the variolites, or can be followed along strike as the pyroclastic breccias. Syn. = Potchefstroom syncline.

Table 2: Major and trace element data for the Hekpoort samples analyzed for this study. Potch. Syn. = Potchefstroom syncline. Eu/Eu* = the value of the Eu anomaly calculated by the formula $[Eu/Eu^*] = [(Eu_N)/((Sm_N * Gd_N)^{0.5})]$ from *Worrall and Pearson (2001)*.

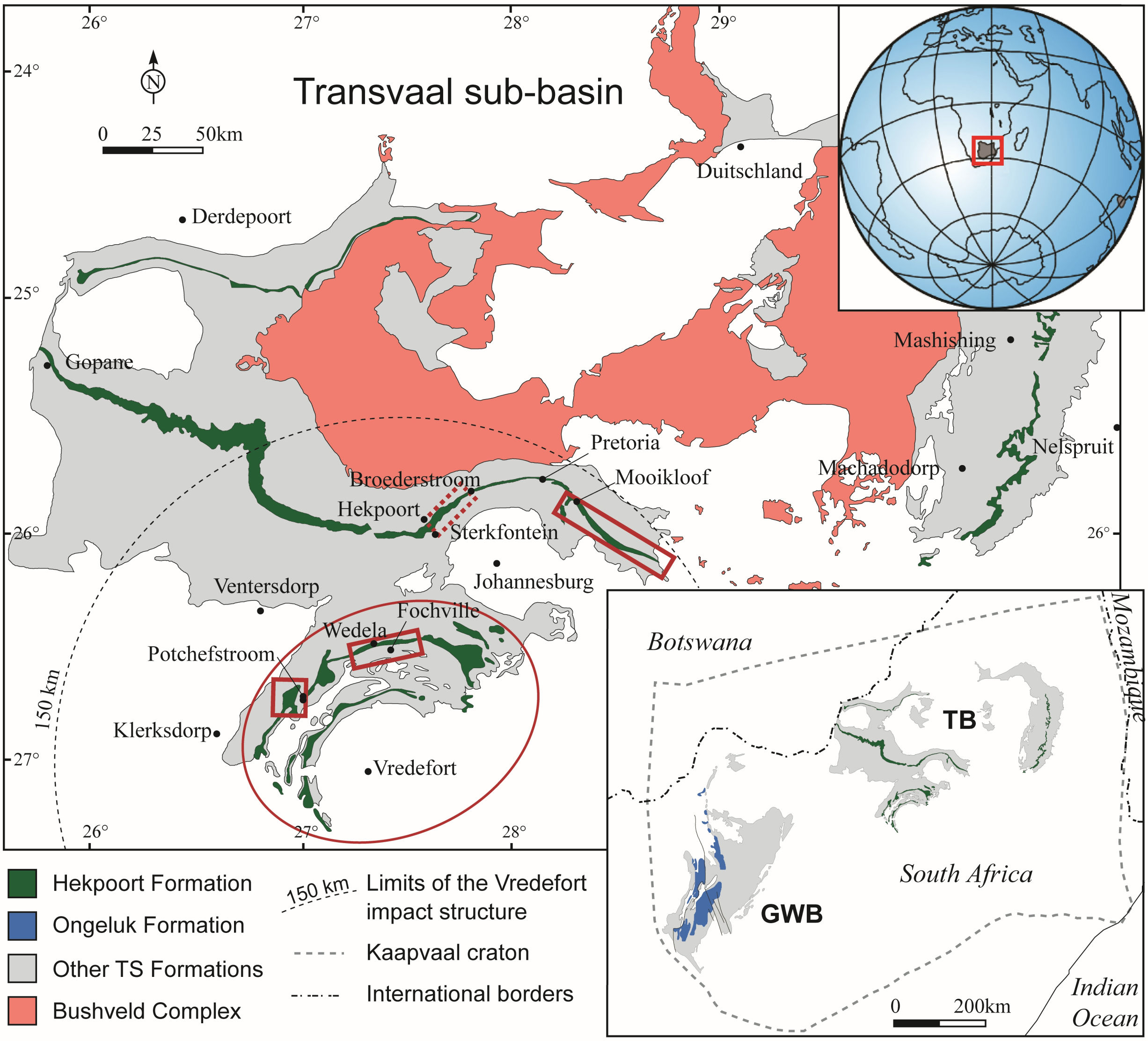

Transvaal sub-basin
0 25 50km
N
26°
27°
28°
29°
24°
25°
26°
27°
Derdepoort
Gopane
Duitschland
Mashishing
Nelspruit
Machadodorp
Pretoria
Mooikloof
Broederstroom
Hekpoort
Sterkfontein
Johannesburg
Ventersdorp
Fochville
Wedela
Potchefstroom
Klerksdorp
Vredefort
150 km
Botswana
Mozambique
TB
GWB
South Africa
Indian Ocean
0 200km
Hekpoort Formation
Ongeluk Formation
Other TS Formations
Bushveld Complex
Limits of the Vredefort impact structure
Kaapvaal craton
International borders

Figure 1

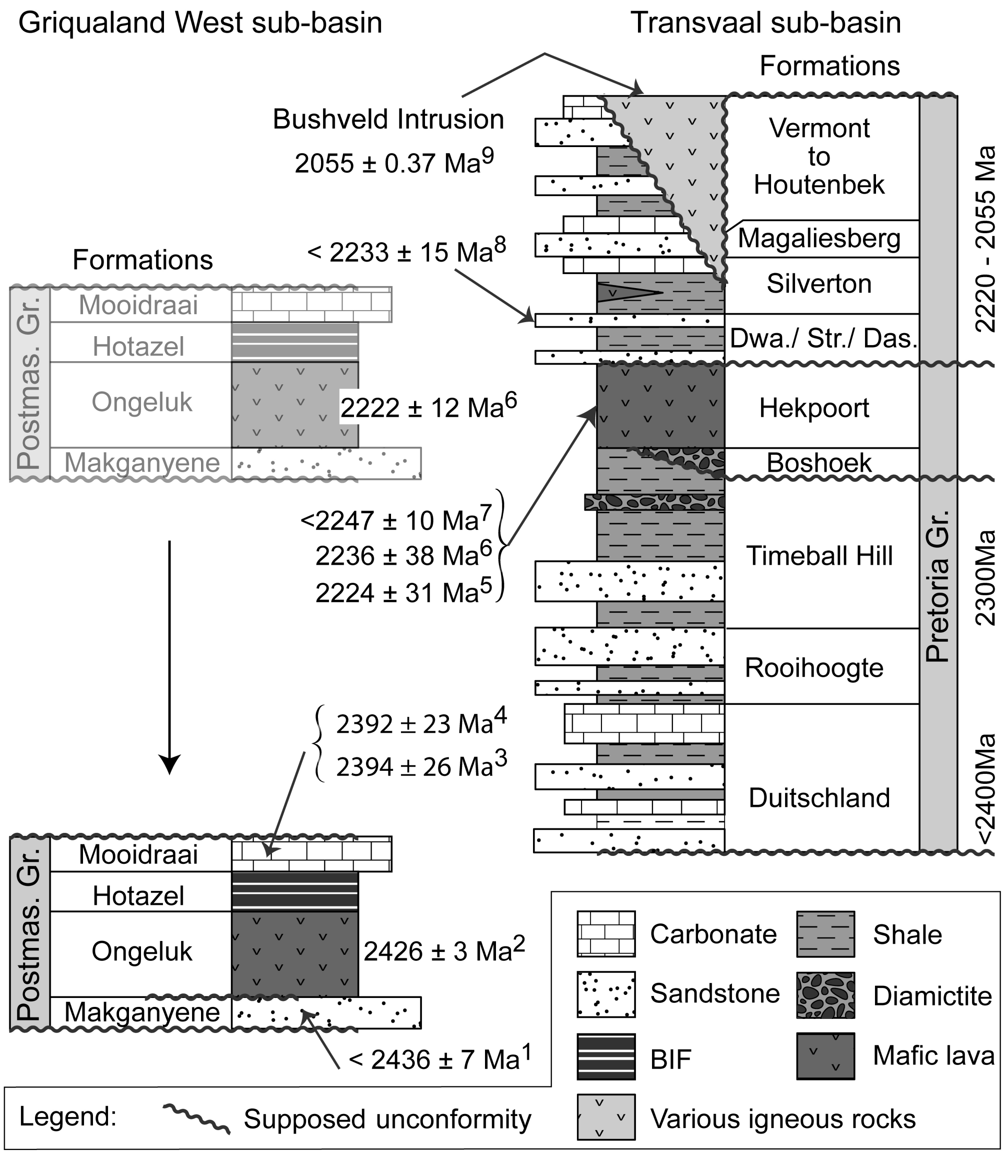

Griqualand West sub-basin
Transvaal sub-basin
Formations
Bushveld Intrusion
2055 ± 0.37 Ma9
Vermont
to
Houtenbek
Magaliesberg
Silverton
Dwa./ Str./ Das.
2220 - 2055 Ma
< 2233 ± 15 Ma8
Formations
Postmas. Gr.
Mooidraai
Hotazel
Ongeluk
2222 ± 12 Ma6
Makganyene
Hekpoort
Boshoek
<2247 ± 10 Ma7
2236 ± 38 Ma6
2224 ± 31 Ma5
Timeball Hill
Pretoria Gr.
2300Ma
Rooihoogte
2392 ± 23 Ma4
2394 ± 26 Ma3
Duitschland
<2400Ma
Postmas. Gr.
Mooidraai
Hotazel
Ongeluk
2426 ± 3 Ma2
Makganyene
< 2436 ± 7 Ma1
Carbonate
Shale
Sandstone
Diamictite
BIF
Mafic lava
Various igneous rocks
Legend:
Supposed unconformity

Figure 2

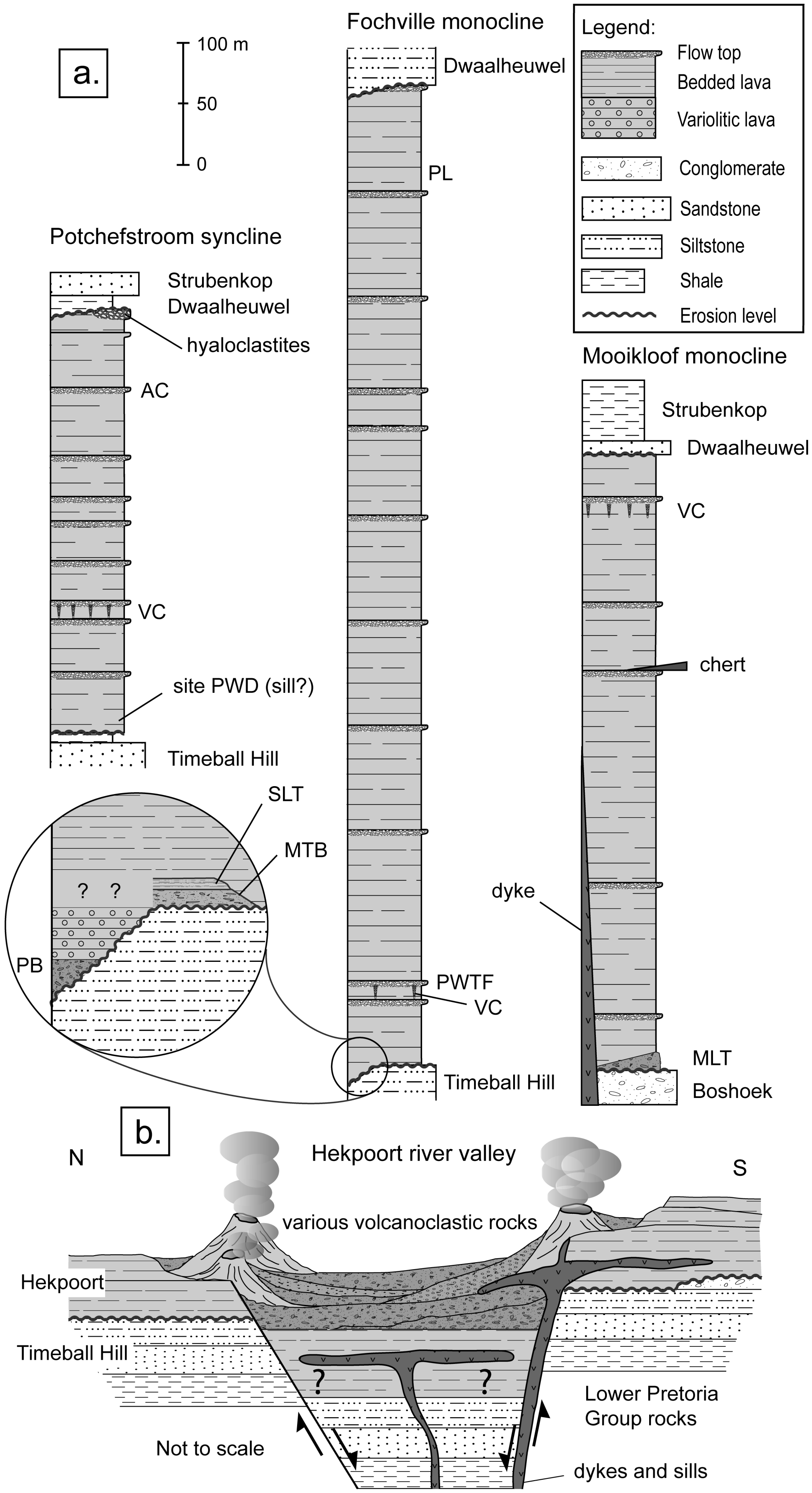
a.
100 m
50
0
Potchefstroom syncline
Strubenkop
Dwaalheuwel
hyaloclastites
AC
VC
site PWD (sill?)
Timeball Hill
SLT
MTB
? ?
PB
Fochville monocline
Dwaalheuwel
PL
PWTF
VC
Timeball Hill
Legend:
Flow top
Bedded lava
Variolitic lava
Conglomerate
Sandstone
Siltstone
Shale
Erosion level
Mooikloof monocline
Strubenkop
Dwaalheuwel
VC
chert
dyke
MLT
Boshoek
b.
N
Hekpoort river valley
S
various volcanoclastic rocks
Hekpoort
Timeball Hill
? ?
Lower Pretoria
Group rocks
Not to scale
dykes and sills

Figure 3

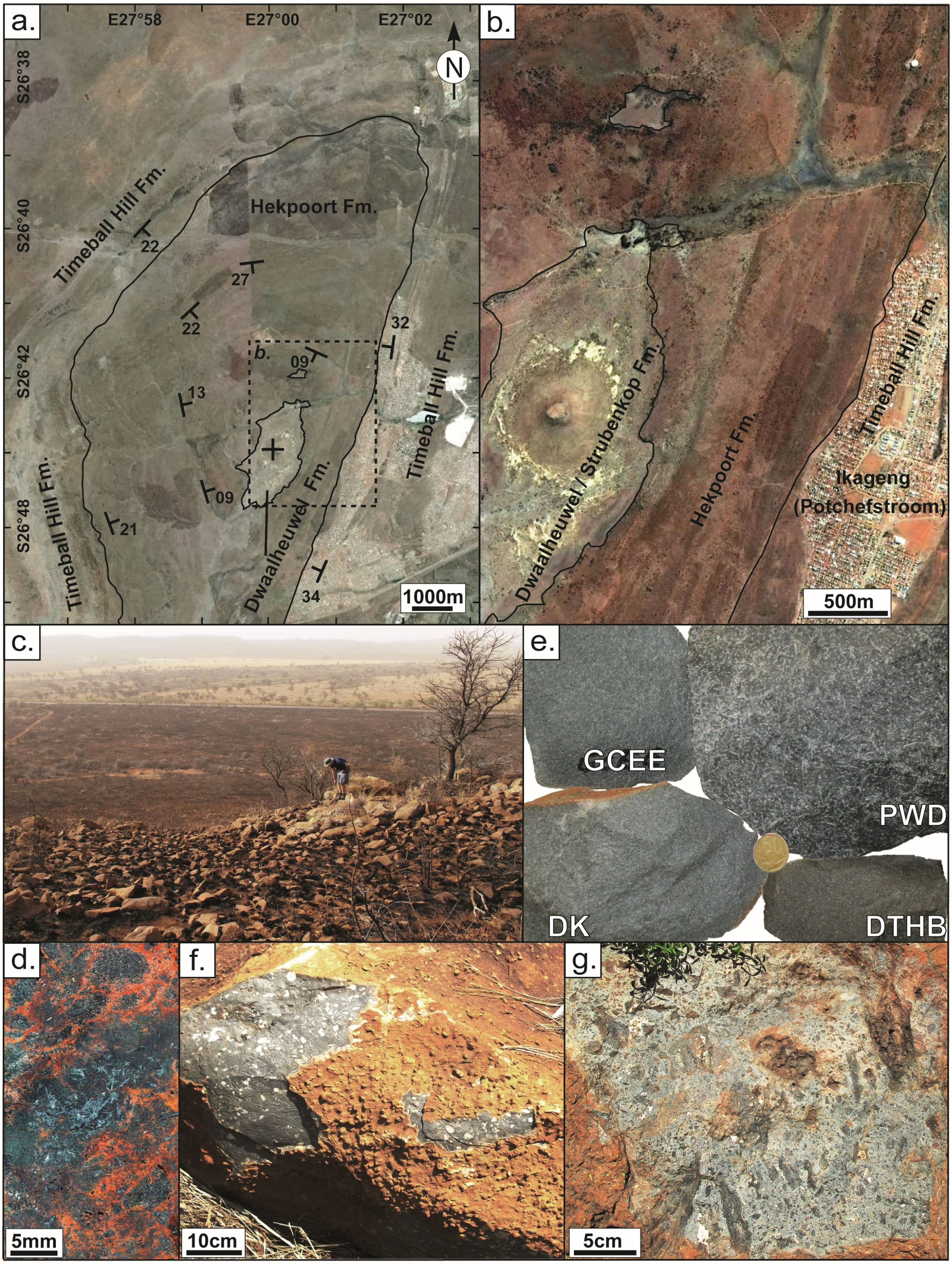

a.
E27°58
E27°00
E27°02
N
S26°38
S26°40
S26°42
S26°48
Timeball Hill Fm.
Hekpoort Fm.
Dwaalheuwel Fm.
b.
22
27
22
32
09
13
09
21
34
1000m
b.
Dwaalheuwel / Strubenkop Fm.
Hekpoort Fm.
Timeball Hill Fm.
Ikageng
(Potchefstroom)
500m
c.
e.
GCEE
PWD
DK
DTHB
d.
5mm
f.
10cm
g.
5cm

Figure 4

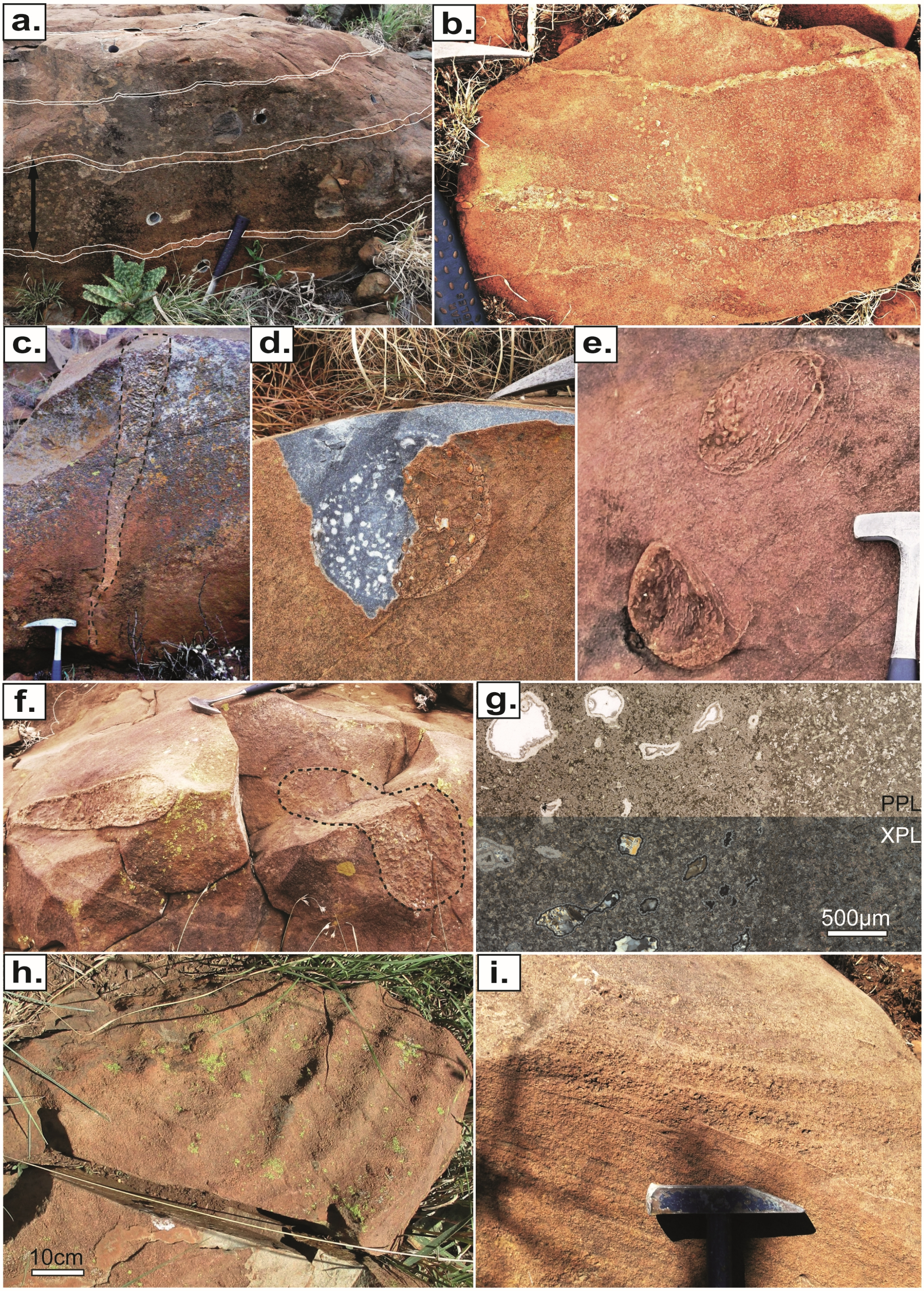

Figure 5a

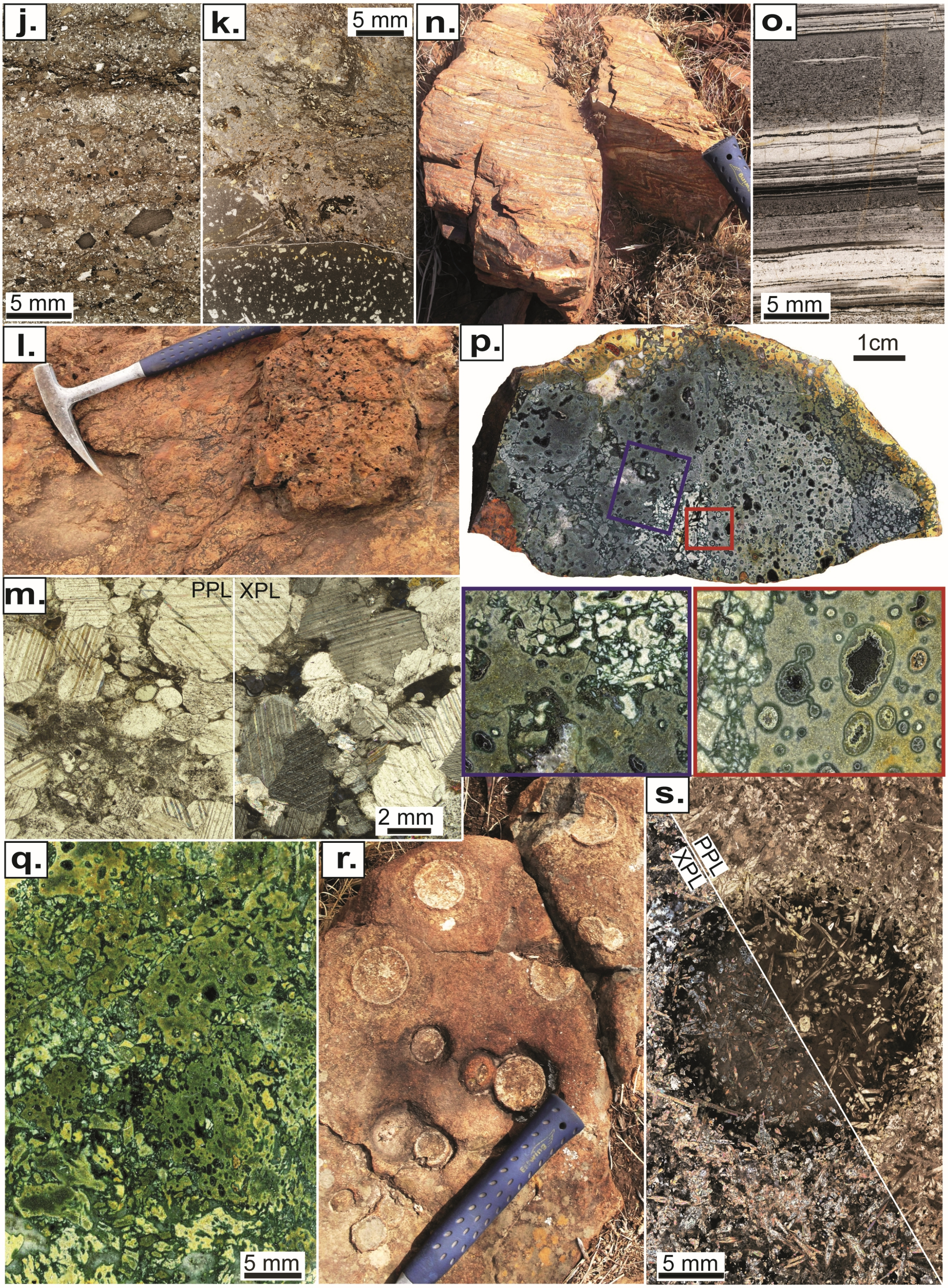

Figure 5b

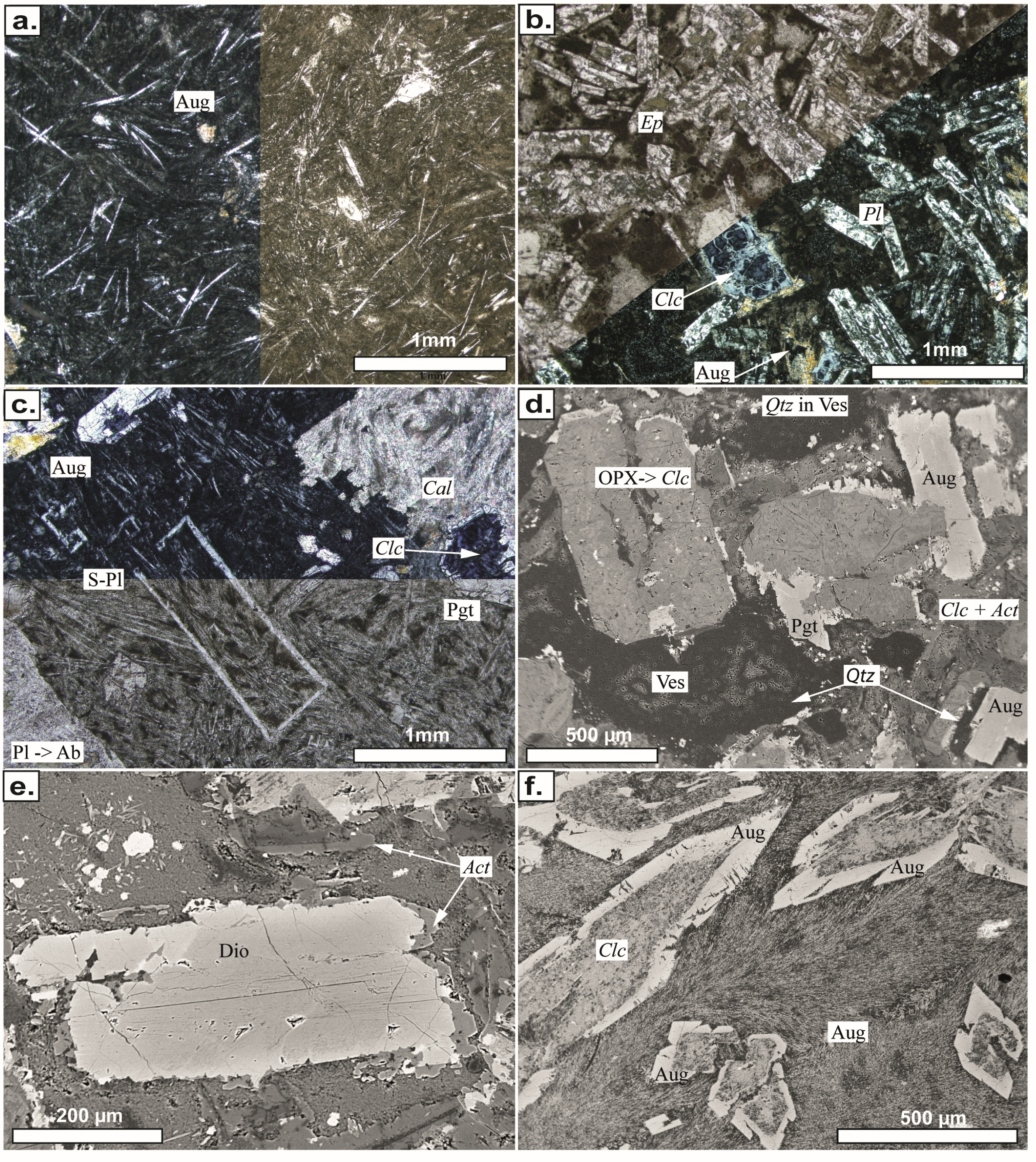
a.
Aug
1mm
b.
Ep
Pl
Clc
Aug
1mm
c.
Aug
Cal
Clc
S-Pl
Pgt
Pl -> Ab
1mm
d.
Qtz in Ves
OPX-> Clc
Aug
Clc + Act
Pgt
Ves
Qtz
Aug
500 µm
e.
Act
Dio
200 µm
f.
Aug
Aug
Clc
Aug
Aug
500 µm

Figure 6

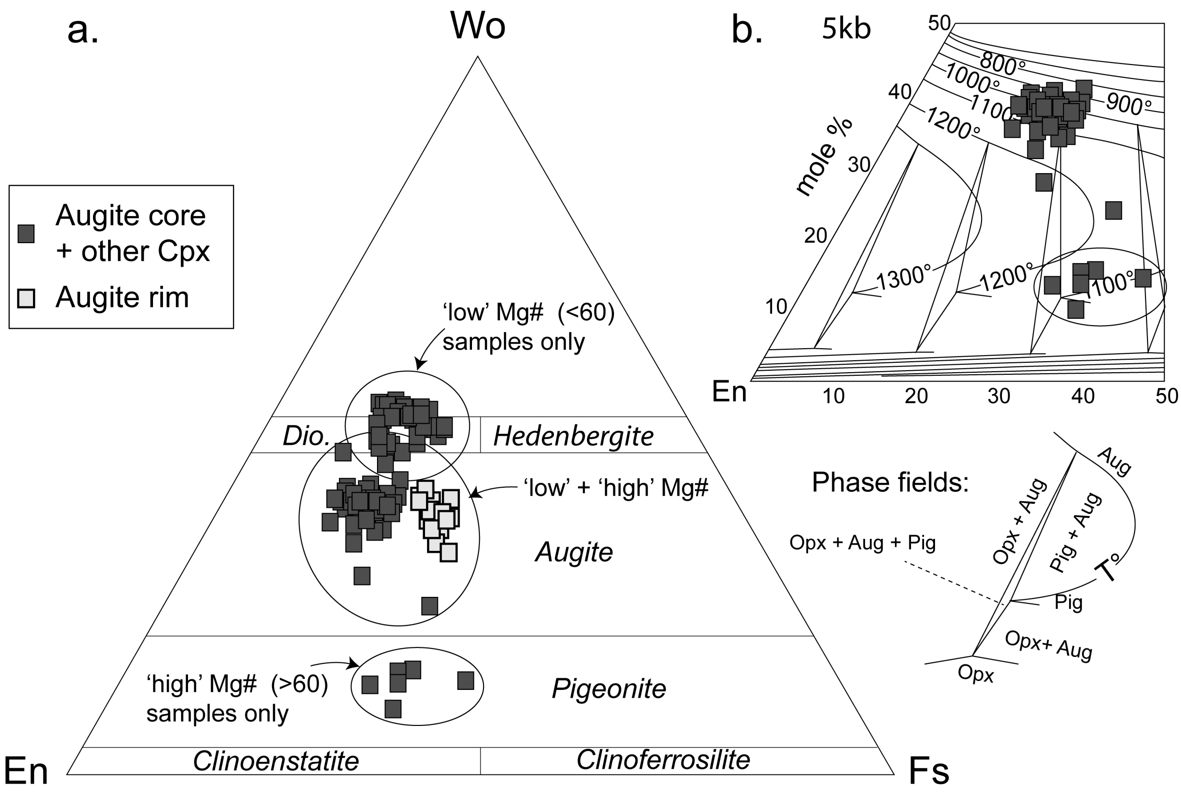

a.
Wo
Augite core
+ other Cpx
Augite rim
'low' Mg# (<60)
samples only
Dio.
Hedenbergite
'low' + 'high' Mg#
Augite
'high' Mg# (>60)
samples only
Pigeonite
En
Clinoenstatite
Clinoferrosilite
Fs
b.
5kb
800°
1000°
1100°
900°
1200°
mole %
1300°
1200°
1100°
En
10
20
30
40
50
Phase fields:
Opx + Aug + Pig
Opx + Aug
Pig + Aug
Aug
T°
Pig
Opx+ Aug
Opx

Figure 7

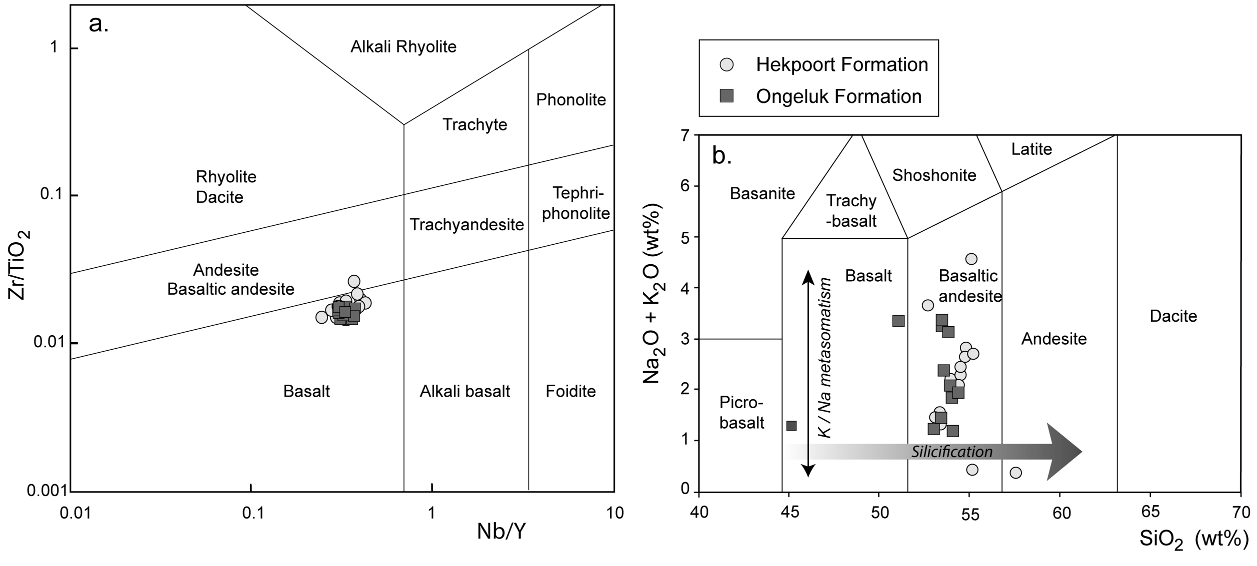
a.
Alkali Rhyolite
Phonolite
Trachyte
Rhyolite
Dacite
Tephri-
phonolite
Trachyandesite
Andesite
Basaltic andesite
Basalt
Alkali basalt
Foidite
Zr/TiO2
Nb/Y
b.
Hekpoort Formation
Ongeluk Formation
Basanite
Trachy
-basalt
Shoshonite
Latite
Basalt
Basaltic
andesite
Andesite
Dacite
Picro-
basalt
K / Na metasomatism
Silicification
Na2O + K2O (wt%)
SiO2 (wt%)

Figure 8

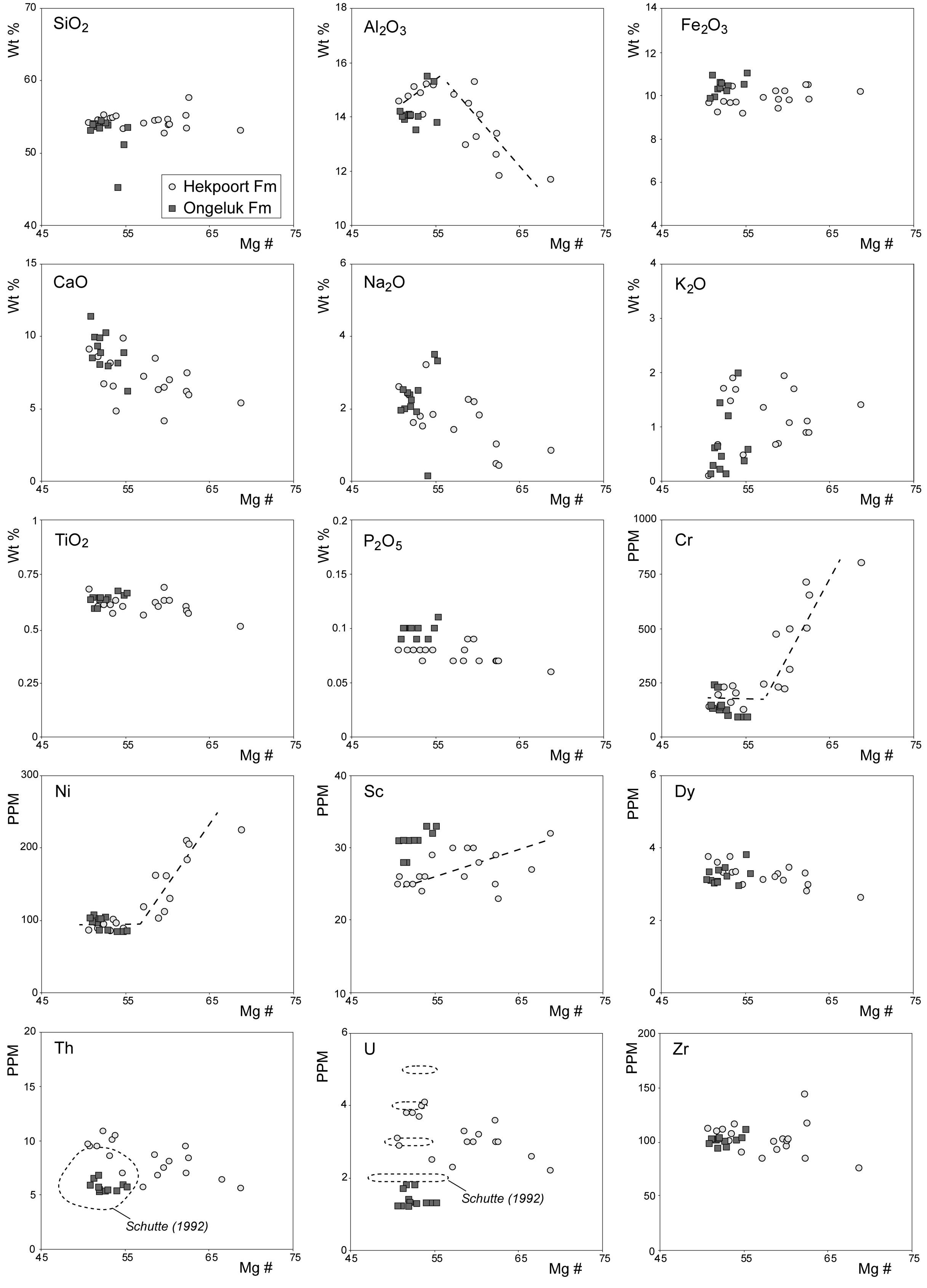
SiO2
Wt %
Hekpoort Fm
Ongeluk Fm
Al2O3
Fe2O3
CaO
Na2O
K2O
TiO2
P2O5
Cr
PPM
Ni
Sc
Dy
Th
U
Zr
Schutte (1992)
Mg #

Figure 9

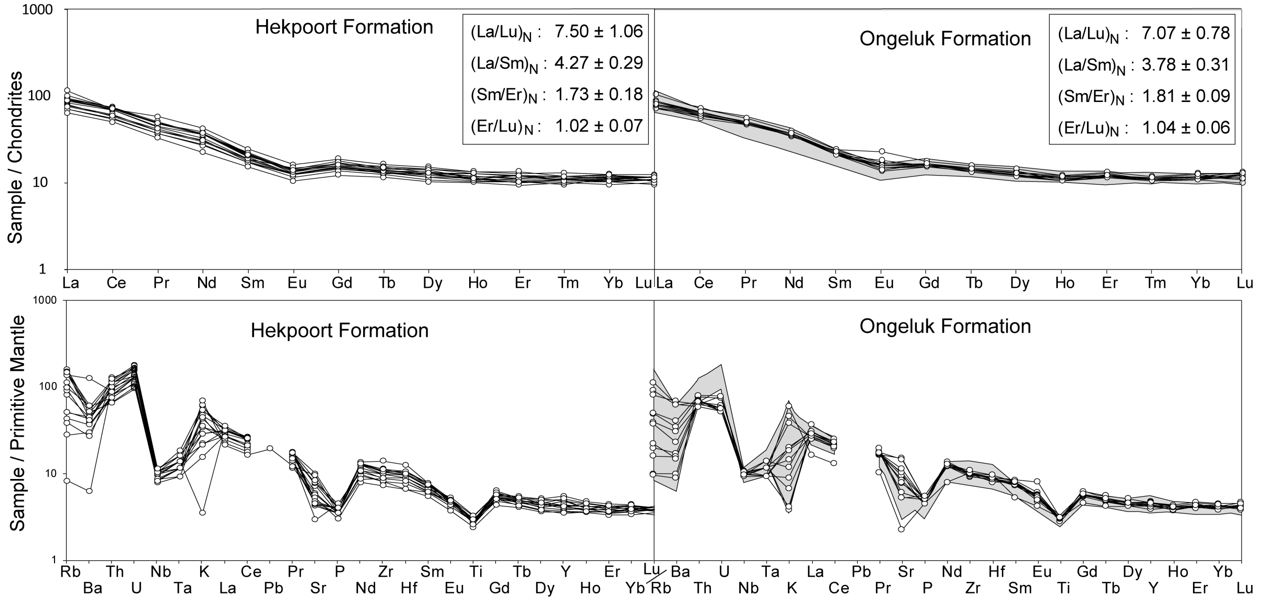

Hekpoort Formation
(La/Lu)N : 7.50 ± 1.06
(La/Sm)N : 4.27 ± 0.29
(Sm/Er)N : 1.73 ± 0.18
(Er/Lu)N : 1.02 ± 0.07
Ongeluk Formation
(La/Lu)N : 7.07 ± 0.78
(La/Sm)N : 3.78 ± 0.31
(Sm/Er)N : 1.81 ± 0.09
(Er/Lu)N : 1.04 ± 0.06
Sample / Chondrites
Sample / Primitive Mantle
1000
100
10
1
La Ce Pr Nd Sm Eu Gd Tb Dy Ho Er Tm Yb Lu
Rb Ba Th U Nb Ta K La Ce Pb Pr Sr P Nd Zr Hf Sm Eu Ti Gd Tb Dy Y Ho Er Yb Lu

Figure 10

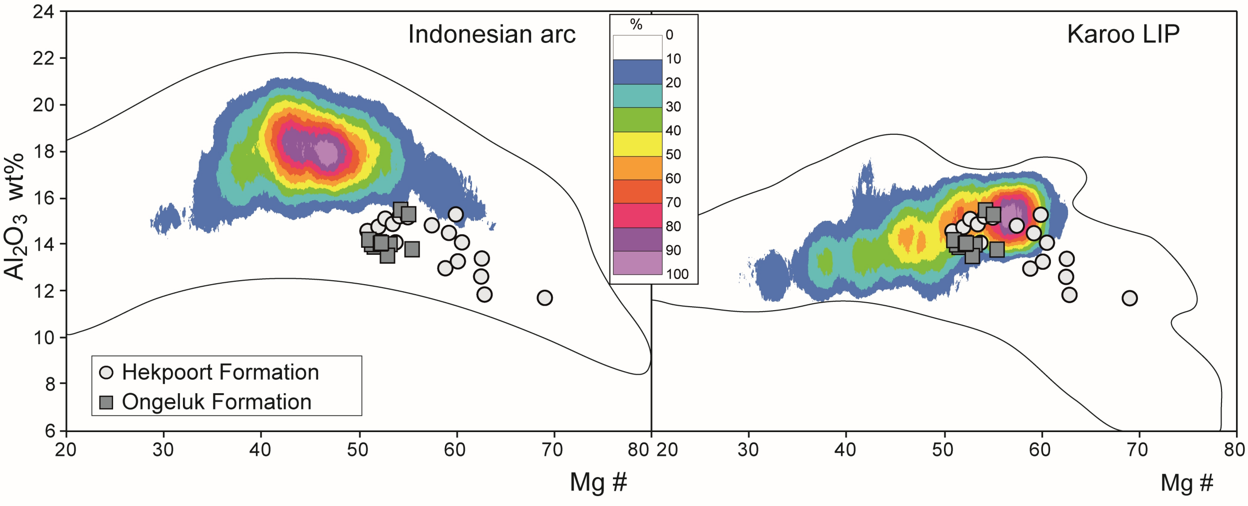

Indonesian arc
Karoo LIP
%
0
10
20
30
40
50
60
70
80
90
100
Al2O3 wt%
Hekpoort Formation
Ongeluk Formation
Mg #
Mg #
24
22
20
18
16
14
12
10
8
6
20
30
40
50
60
70
80

Figure 11

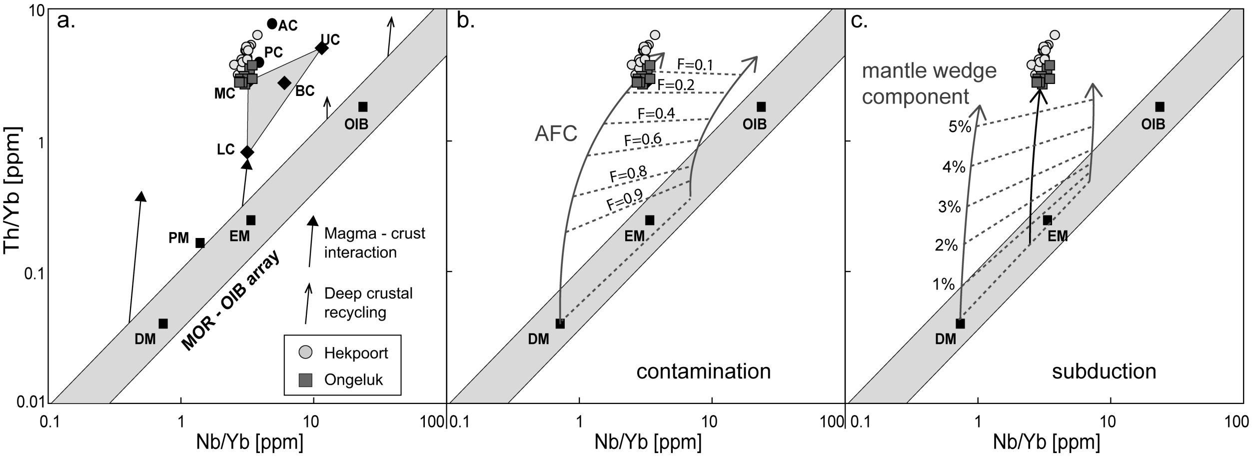

a.
b.
c.
Th/Yb [ppm]
Nb/Yb [ppm]
AC
UC
PC
MC
BC
LC
OIB
PM
EM
DM
MOR - OIB array
Magma - crust interaction
Deep crustal recycling
Hekpoort
Ongeluk
AFC
F=0.1
F=0.2
F=0.4
F=0.6
F=0.8
F=0.9
contamination
mantle wedge component
5%
4%
3%
2%
1%
subduction

Figure 12

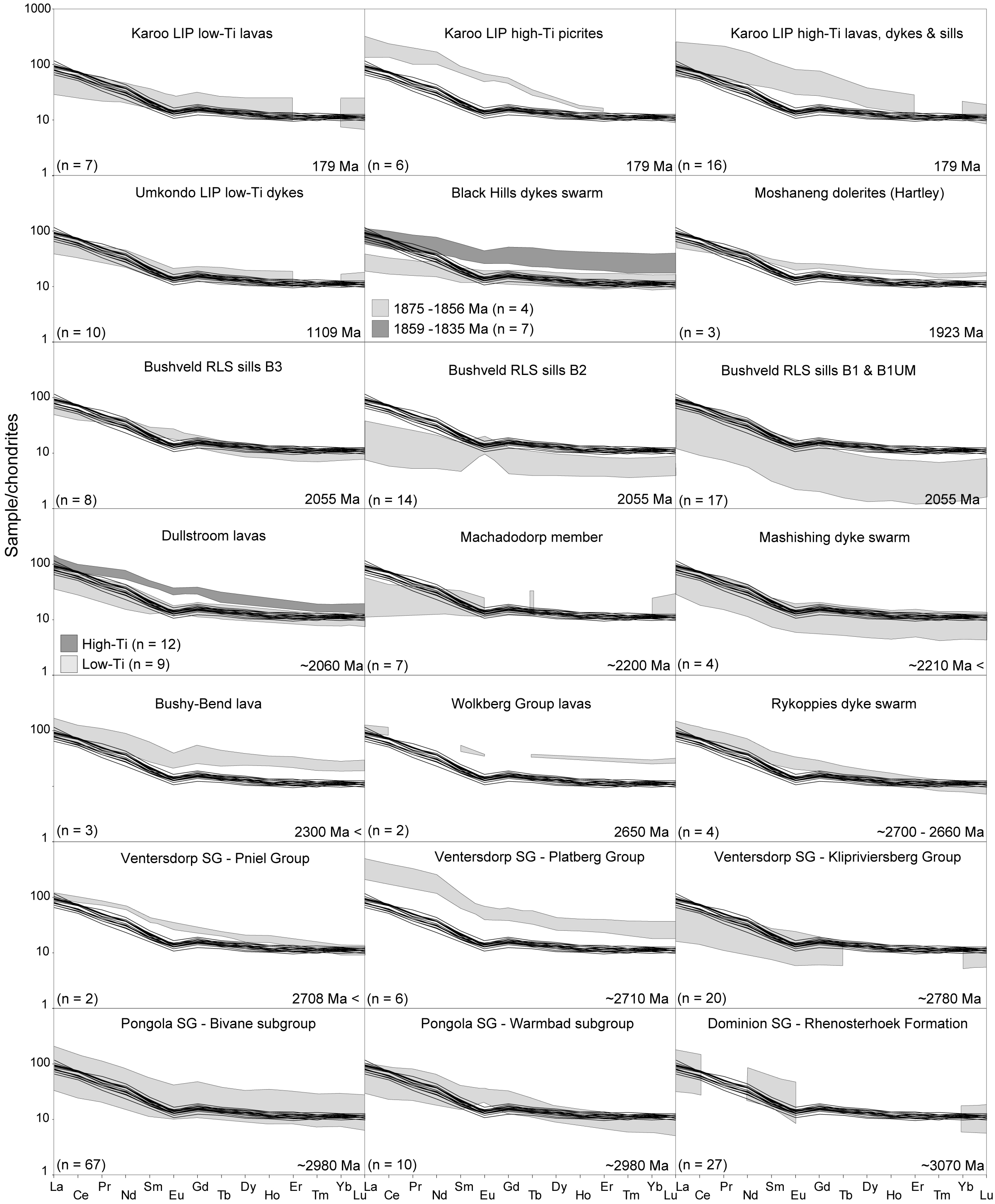

Karoo LIP low-Ti lavas
(n = 7)
179 Ma
Karoo LIP high-Ti picrites
(n = 6)
179 Ma
Karoo LIP high-Ti lavas, dykes & sills
(n = 16)
179 Ma
Umkondo LIP low-Ti dykes
(n = 10)
1109 Ma
Black Hills dykes swarm
1875 -1856 Ma (n = 4)
1859 -1835 Ma (n = 7)
Moshaneng dolerites (Hartley)
(n = 3)
1923 Ma
Bushveld RLS sills B3
(n = 8)
2055 Ma
Bushveld RLS sills B2
(n = 14)
2055 Ma
Bushveld RLS sills B1 & B1UM
(n = 17)
2055 Ma
Dullstroom lavas
High-Ti (n = 12)
Low-Ti (n = 9)
~2060 Ma
Machadodorp member
(n = 7)
~2200 Ma
Mashishing dyke swarm
(n = 4)
~2210 Ma <
Bushy-Bend lava
(n = 3)
2300 Ma <
Wolkberg Group lavas
(n = 2)
2650 Ma
Rykoppies dyke swarm
(n = 4)
~2700 - 2660 Ma
Ventersdorp SG - Pniel Group
(n = 2)
2708 Ma <
Ventersdorp SG - Platberg Group
(n = 6)
~2710 Ma
Ventersdorp SG - Klipriviersberg Group
(n = 20)
~2780 Ma
Pongola SG - Bivane subgroup
(n = 67)
~2980 Ma
Pongola SG - Warmbad subgroup
(n = 10)
~2980 Ma
Dominion SG - Rhenosterhoek Formation
(n = 27)
~3070 Ma
Sample/chondrites
1000
100
10
1
La Ce Pr Nd Sm Eu Gd Tb Dy Ho Er Tm Yb Lu

Figure 13

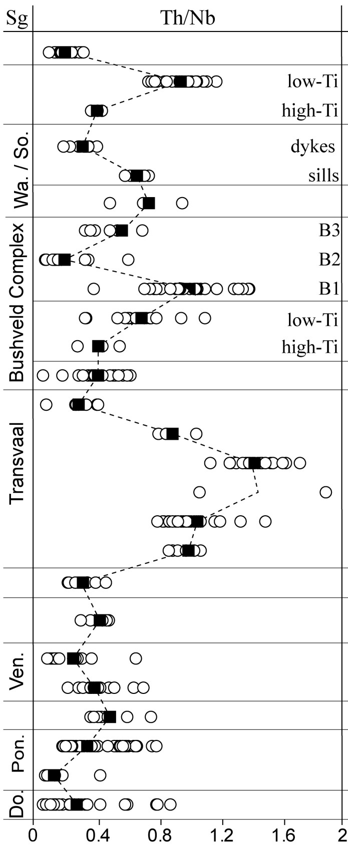

Mafic units	n	Age (Ma)	εNd(t)	References
Karoo LIP	31	179	*	Jourdan et al. (2007)
Umkondo LIP	20 3	1109	- - 3.7	Bullen et al. (2012); own data
Black Hills dykes swarm	11 4	1875 to 1835	-	Hanson et al. (2004); Olsson et al. (2016); own data
Hartley dolerites	3	1923	-	Hanson et al. (2004)
Rustenberg Layered Suite sills	8 14 31	2055	- 6.8 - 6.8 - 5.5	Maier et al. (2000); Barnes et al. (2010); own data
Uitkomst Complex	16 3	2058	- -	Gomwe (2006); Wabo et al. (2016)
Dullstroom lavas -	21	2060 (?)	- 9.6	Buchanan et al. (1999)
Machadodorp member	7	2250 <	-	Crow & Condie (1990); Wabo et al. (subm)
Mashishing dyke swarm	4	~2208	-	Wabo et al. (subm)
Hekpoort Formation	16	~2225	-	this paper
Bushy-Bend lava	2	2300 <	-	own data
Ongeluk Formation	27	~2426	2.8	Schutte (1992); this paper; own data
Westerberg sills	6	~2446	-	own data
Wolkberg Group	9	2710 <	-	Crow & Condie (1990); Bosch (1992)
Rykoppies dyke swarm	5	~2700 to 2660	-	Klausen et al. (2010)
Pniel & Platberg groups	20	~2710	- 3.3	Crow & Condie (1988); Nelson et al. (1992);
Klipriviersberg Group	24	~2780	0.0	Marsh et al. (1992); Altermann & Lenhardt (2012)
Badplaas dyke swarm	7	~2980	-	Klausen et al. (2010)
Bivane Subgroup	67	~2980	-3.3	Armstrong et al. (1986); Bowen et al. (1986);
Warmbad Subgroup	10			Grant (2003); Mukasa et al. (2013)
Rhenosterhoek Fm	27	~3070	0.0	Crow & Condie (1987); Marsh et al. (1989)

Figure 14

	Region	Lat. (S)	Long. (E)
Hyaloclastites	Potch. Syn.	26°42'53.12"	26°59'14.66"
Interbedded sedimentary units	Mooikloof *	25°51'13.69"	28°22'06.48"
Pahoehoe lava	Fochville *	26°28'52.01"	27°23'14.84"
Paleo-weathered flow tops	Fochville	26°27'09.82"	27°22'29.40"
Variolitic lava flows	Fochville	26°28'25.91"	27°22'02.74"
Vesicle cylinders	Potch. Syn.	26°40'28.67"	26°59'11.02"
	Mooikloof *	25°51'21.60"	28°22'29.40"
Volcanoclastic rocks:			
Stratified lapilli-tuff	Fochville	26°28'16.40"	27°23'12.27"
	Fochville *	26°27'04.90"	27°26'17.40"
Massive lapilli-tuff	Mooikloof *	25°52'35.10"	28°22'06.70"
	Hekpoort RV*	25°53'13.01"	27°42'46.48"
Massive tuff-breccias	Fochville	26°28'16.40"	27°23'12.27"
Pyroclastic breccias	Fochville	26°28'29.64"	27°21'34.23"
	Hekpoort RV	25°50'42.36"	27°46'02.73"
Clast of 3 meter large	Hekpoort RV	25°50'39.10"	27°46'05.90"

Table 1

Table 2

	Formation	Hekpoort	Hekpoort	Hekpoort	Hekpoort	Hekpoort	Hekpoort	Hekpoort	Hekpoort	Hekpoort	Hekpoort	Hekpoort	Hekpoort	Hekpoort
	Region	Potch. Syn.	Potch. Syn.	Potch. Syn.	Potch. Syn.	Fochville	Fochville	Fochville	Fochville	Mooikloof	Mooikloof	Mooikloof	Mooikloof	Mooikloof
Sample	Precision	PWB	PWC	PWF	PWD	DK	GVAR 2	DTHB	DTH-C	HK154	GCEA	GCEB	GCED	GCEE
Material	accuracy	Lava	Lava	Lava	Lava	Aphanitic lava	Variolitic lava	Lava	Lava	Volcanoclastite	Volcanoclastit	Lava	Lava	Lava
Lat. (S)		26°42'44.32"	26°42'54.63"	26°40'28.28"	26°42'25.83"	26°29'57.98"	26°28'19.26"	26°27'07.10"	26°27'08.26"	25°52'35.10"	25°52'35.00"	25°51'10.70"	25°51'11.78"	25°51'06.25"
Long. (E)		26°58'54.54"	26°58'58.89"	26°58'57.97"	27°01'21.52"	27°22'40.14"	27°22'01.88"	27°26'22.15"	27°26'15.21"	28°22'06.70"	28°22'06.20"	28°22'33.40"	28°22'05.15"	28°22'08.65"
SiO_2	0.01%	53.14	54.54	52.75	54.19	55.24	54.45	54.56	55.13	55.18	57.62	53.38	54.79	53.43
TiO_2	0.01%	0.51	0.6	0.69	0.68	0.61	0.62	0.6	0.63	0.6	0.57	0.6	0.61	0.58
Al_2O_3	0.01%	11.69	14.49	15.28	14.57	15.11	13	14.76	15.2	12.6	11.84	15.17	14.88	13.38
Fe_2O_3t	0.04%	10.19	9.41	10.21	9.67	9.73	10.22	9.23	9.7	10.51	9.84	9.18	9.65	10.49
MnO	0.01%	0.15	0.16	0.17	0.13	0.12	0.16	0.14	0.16	0.14	0.13	0.16	0.15	0.17
MgO	0.01%	11.32	6.81	7.61	5.01	5.41	7.3	4.99	5.72	8.74	8.3	5.6	5.54	8.76
CaO	0.01%	5.39	6.32	4.16	9.13	6.7	8.51	8.61	4.84	6.18	5.96	9.88	8.17	7.47
Na_2O	0.01%	0.84	2.25	2.19	2.6	1.61	2.1	2.41	3.21	0.47	0.42	1.84	1.78	1.02
K_2O	0.01%	1.41	0.7	1.94	0.11	1.71	0.69	0.68	1.69	0.9	0.9	0.49	1.48	1.11
P_2O_5	0.01%	0.06	0.09	0.09	0.08	0.08	0.08	0.08	0.08	0.07	0.07	0.08	0.08	0.07
Cr_2O_3	0.00%	0.117	0.033	0.032	0.02	0.033	0.07	0.028	0.029	0.104	0.095	0.018	0.023	0.073
LOI	-	4.9	4.4	4.6	3.6	3.4	2.6	3.7	3.4	4.2	4	3.4	2.6	3.2
Total	0.01%	99.7	99.79	99.69	99.82	99.78	99.77	99.8	99.77	99.73	99.75	99.81	99.78	99.75
Mg#	-	68.77	58.92	59.63	50.66	52.42	58.60	51.72	53.89	62.24	62.57	54.73	53.22	62.34
Ni (XRF)	20 ppm	225	103	112	86	94	163	89	96	210	205	89	85	183
Sc (XRF)	1 ppm	32	30	30	25	25	26	25	26	25	23	29	26	29
Rb	0.1 ppm	89.7	26.2	82.9	5	90.6	27.9	23.4	59.5	31	30.9	16.9	83.5	55.4
Ba	1 ppm	354	251	862	43	284	160	185	416	290	308	205	355	262
Th	0.2 ppm	5.6	6.8	7.5	9.7	10.9	8.7	9.5	10.5	9.5	8.4	7	8.6	7
U	0.1 ppm	2.2	3	3	3.1	3.8	3.3	3.8	4.1	3.6	3	2.5	3.7	3
Nb	0.1 ppm	4.7	5.2	5.9	6.3	6.7	5.8	6.2	6.8	5.9	5.7	5.1	6.2	4.9
Ta	0.1 ppm	0.4	0.5	0.6	0.6	0.7	0.6	0.6	0.7	0.5	0.6	0.4	0.5	0.5
La	0.1 ppm	15.4	18.7	18.3	23	22.2	19.1	21.6	24.3	22	21.2	19.1	22.3	17
Ce	0.1 ppm	31.3	38.1	37	46.2	45.5	37.3	44.4	44.8	44.3	43.5	36	42.9	33.9
Pb	0.1 ppm	ND	ND	ND	ND	ND	7.5	ND	ND	ND	ND	ND	ND	ND
Pr	0.02 ppm	3.11	3.71	3.96	4.75	4.54	4	4.56	4.6	4.56	4.52	3.75	4.25	3.48
Sr	0.5 ppm	116.2	64.8	172.8	105.3	219.6	124.8	185.8	99.9	102.9	93.7	97.3	170.7	97.3
Nd	0.3 ppm	10.7	14.1	14.5	17.2	17.2	15.6	16.9	17.6	18.2	17.2	14.9	17	12.8
Zr	0.1 ppm	74.9	91.9	102.2	111.4	110.7	101.1	109.2	116.1	143.9	116.5	90.1	100.8	84.4
Hf	0.1 ppm	2	2.7	2.7	3.1	3.2	3.1	2.9	3	3.8	3.2	2.5	2.9	2.3
Sm	0.05 ppm	2.38	2.82	2.91	3.39	3.24	3.05	3.17	3.26	3.32	3.32	2.68	3.08	2.6
Eu	0.02 ppm	1	1	1	1	1	0.79	1	1	1	1	1	1	1
Gd	0.05 ppm	3	3	3	3	3	3.31	4	3	3	3	3	4	3
Tb	0.01 ppm	0.44	0.49	0.54	0.59	0.52	0.54	0.55	0.57	0.53	0.51	0.5	0.56	0.47
Dy	0.05 ppm	2.63	3.27	3.1	3.74	3.32	3.19	3.59	3.34	3.29	2.97	2.98	3.74	2.79
Y	0.1 ppm	15	16.6	18.3	20	17.2	18.4	20.7	21.3	17.1	15.9	17.8	22.7	15.4
Ho	0.02 ppm	0.57	0.61	0.66	0.72	0.63	0.68	0.63	0.73	0.73	0.64	0.59	0.76	0.58
Er	0.03 ppm	1.56	1.84	2.01	2	1.67	1.98	2	2	1.96	1.65	1.7	2.1	1.71
Tm	0.01 ppm	0.26	0.29	0.28	0.3	0.27	0.29	0.3	0.31	0.28	0.28	0.29	0.34	0.25
Yb	0.05 ppm	1.62	1.75	1.83	2.02	1.75	1.83	1.98	2.07	1.88	1.75	1.79	2.12	1.9
Lu	0.01 ppm	0.25	0.28	0.3	0.29	0.27	0.28	0.29	0.29	0.29	0.24	0.27	0.26	0.27
Co	0.2 ppm	51.7	34.4	39.4	38.7	35.3	41.9	35.5	38.4	55.1	40.3	38.3	39.1	41.7
Cs	0.1 ppm	1.9	1.2	1.9	0.5	2.7	0.9	0.8	0.8	1.4	1.2	0.3	1.3	2.5
Ga	0.5 ppm	11.7	14.7	15.5	16.1	16.8	15.3	16.3	14.1	14.4	13.8	15.9	16	13.8
V	8 ppm	194	180	193	186	171	188	178	188	172	162	189	183	191
Eu/Eu*	-	0.76	0.74	0.84	0.74	0.74	0.75	0.71	0.76	0.72	0.70	0.78	0.76	0.77

	Hekpoort	Hekpoort	Hekpoort	Ongeluk	Ongeluk	Ongeluk	Ongeluk	Ongeluk	Ongeluk	Ongeluk	Ongeluk	Ongeluk	Ongeluk	Ongeluk	Ongeluk
	Mooikloof	Mooikloof	Mooikloof	Postmasburg	Postmasburg	Postmasburg	Postmasburg	Postmasburg	Postmasburg	Postmasburg	Postmasburg	Postmasburg	Postmasburg	Postmasburg	Postmasburg
Sample	ATS30	ATD07	WA12/30	ONG-A2	ONG-A4	ONG-B2	ONG-B3	ONG-C1	ONG-D2	ONG-D3	ONG-E1	ONG-E3	ONG-IF	ONG-PIL2	ONG-PIL3
Material	Lava	Lava	Lava	Lava	Lava	Lava	Lava	Lava	Lava	Lava	Lava	Lava	Pillow rim	Pillow	Pillow
Lat. (S)	25°50'48.40"	25°51'54.80"	25°52'16.70"	28°53'47.20"	28°53'47.20"	28°53'31.50"	28°53'31.50"	28°53'37.00"	28°53'34.70"	28°53'34.70"	28°53'41.00"	28°53'41.00"	28°53'48.26"	28°53'48.26"	28°53'48.26"
Long. (E)	28°21'58.00"	28°22'58.60"	28°22'17.40"	22°49'12.30"	22°49'12.30"	22°51'46.90"	22°51'46.90"	22°53'06.70"	22°56'04.20"	22°56'04.20"	22°56'36.80"	22°56'36.80"	22°49'16.20"	22°49'16.20"	22°49'16.20"
SiO_2	53.99	54.13	54.86	53.48	53.83	54.03	53.58	53.93	53.03	54.07	53.44	54.4	45.15	51.06	53.51
TiO_2	0.63	0.56	0.57	0.64	0.64	0.59	0.59	0.64	0.63	0.63	0.63	0.64	0.67	0.65	0.66
Al_2O_3	14.08	14.82	14.09	14.07	14	13.9	14.06	14	14.19	13.49	14.02	14.06	15.48	15.29	13.77
Fe_2O_3t	9.8	9.88	10.45	10.61	10.46	9.95	10.28	10.95	9.91	10.22	10.34	10.6	13.73	10.51	11.05
MnO	0.14	0.16	0.16	0.13	0.13	0.14	0.15	0.14	0.14	0.14	0.15	0.15	0.13	0.14	0.13
MgO	7.5	6.66	6.07	5.79	5.94	5.3	5.55	5.78	5.18	5.75	5.65	5.82	8.17	6.44	6.89
CaO	7.01	7.22	6.57	8.03	7.95	9.94	9.31	8.49	11.38	10.25	9.9	8.84	8.13	8.87	6.22
Na_2O	1.81	1.41	1.51	2.36	2.48	1.98	2.42	2.51	1.94	1.9	2.04	2.22	0.13	3.5	3.31
K_2O	1.08	1.36	1.9	1.43	1.2	0.61	0.63	0.28	0.12	0.13	0.21	0.45	1.99	0.37	0.58
P_2O_5	0.07	0.07	0.07	0.1	0.1	0.1	0.1	0.1	0.09	0.09	0.1	0.1	0.09	0.1	0.11
Cr_2O_3	0.045	0.035	0.034	0.018	0.014	0.035	0.033	0.019	0.021	0.018	0.02	0.021	0.013	0.013	0.013
LOI	3.6	3.5	3.5	3.1	3	3.2	3.1	2.9	3.1	3.1	3.3	2.5	6	2.8	3.5
Total	99.75	99.78	99.77	99.74	99.75	99.79	99.78	99.77	99.81	99.8	99.79	99.77	99.73	99.77	99.76
Mg#	60.27	57.19	53.51	51.96	52.95	51.35	51.69	51.13	50.88	52.72	51.99	52.11	54.11	54.84	55.27
Ni (XRF)	130	118	101	86	86	107	97	98	103	104	102	102	84	84	85
Sc (XRF)	28	30	24	31	31	28	28	31	31	31	31	31	33	32	33
Rb	48.7	67.9	96.2	54.9	48.9	29.6	30.4	11.9	6	5.8	9.7	23.8	71.6	13.3	22.7
Ba	300	346	375	426	470	236	278	117	68	61	107	210	309	102	157
Th	8.1	5.7	10.1	5.7	5.4	6.5	6.8	6	5.9	5.3	5.6	5.3	5.3	5.9	5.7
U	3.2	2.3	4	1.4	1.3	1.7	1.8	1.2	1.2	1.8	1.2	1.3	1.3	1.3	1.3
Nb	6.2	5	6.6	5.8	5.6	6.2	6.4	5.9	5.7	5.8	5.6	6.1	6.3	6.2	5.8
Ta	0.7	0.5	0.8	0.5	0.5	0.5	0.4	0.4	0.6	0.4	0.5	0.5	0.5	0.6	0.4
La	20	17	21.6	17.8	17.9	21.1	20.8	20.9	19.6	19.5	17.3	18.7	20.5	25.1	19.6
Ce	42.8	34.2	44.7	34.7	36.8	39.2	39.6	40.7	38.9	37.5	36.4	36.2	38.8	44	40.3
Pb	ND	ND	ND	ND	ND	ND	ND	ND	ND	ND	ND	ND	ND	ND	ND
Pr	4.11	3.45	4.48	4.39	4.48	4.6	4.74	4.63	4.4	4.56	4.52	4.57	4.52	5.22	4.66
Sr	130.6	126.5	159.5	330.9	206.8	132.9	169.7	320.5	184.6	173.1	224.1	248.1	26.2	116.9	115.1
Nd	15.7	13.2	17.3	16.4	17.6	17.3	17.4	16.1	16.6	17.7	16.6	17.7	17.1	18.4	17.3
Zr	102.1	83.9	107.2	94.7	96	104	102	103.2	99.6	101.9	103.9	104.2	103	104.3	112.4
Hf	2.7	2	2.9	2.6	2.5	2.6	2.6	2.7	2.7	2.4	2.6	2.6	2.7	2.7	2.9
Sm	2.93	2.66	3.06	3.16	3.24	3.28	3.34	3.6	3.16	3.47	3.2	3.44	3.17	3.66	3.49
Eu	0.76	0.74	1	0.87	0.8	0.92	0.88	1.01	0.96	0.93	0.92	0.87	1.07	1.34	0.83
Gd	3.09	2.97	3	3.19	3.16	3.38	3.23	3.31	3.41	3.41	3.37	3.38	3.21	3.65	3.41
Tb	0.52	0.51	0.52	0.51	0.51	0.54	0.54	0.55	0.53	0.56	0.52	0.53	0.5	0.6	0.55
Dy	3.46	3.11	3.31	3.11	3.23	3.14	3.08	3.33	3.15	3.43	3.1	3.37	3.02	3.73	3.3
Y	17.8	20.2	17.6	16	17.9	18.4	17.2	19	18	17.2	18.9	19.5	17.1	19.2	18.8
Ho	0.67	0.64	0.67	0.65	0.6	0.6	0.66	0.68	0.6	0.62	0.66	0.61	0.6	0.69	0.66
Er	1.82	1.77	1.9	1.91	1.96	2.05	2.13	1.91	1.95	2.01	1.97	2.02	1.87	2.2	2
Tm	0.29	0.28	0.31	0.28	0.29	0.28	0.28	0.29	0.29	0.28	0.3	0.28	0.27	0.31	0.3
Yb	1.94	1.84	1.92	1.85	1.94	1.87	1.85	1.95	2.01	1.82	2.01	1.99	1.81	2.14	2.08
Lu	0.27	0.27	0.29	0.3	0.29	0.29	0.3	0.31	0.27	0.3	0.3	0.3	0.25	0.32	0.28
Co	40.5	38.7	38.5	39.9	41.2	38.1	40.3	45.7	36.3	44.5	41.6	44	53.4	56.6	61.1
Cs	1.4	2.5	3.3	1	1.1	0.4	0.6	0.3	0.2	0.3	0.4	0.6	0.3	0.2	0.2
Ga	15	15.1	14.3	14.3	13.1	14.2	14.5	14.4	15.1	14.9	14.9	14.8	17.4	15.8	11.1
V	192	185	161	194	197	176	182	197	194	196	192	198	203	207	198
Eu/Eu*	0.77	0.80	0.72	0.83	0.76	0.84	0.81	0.89	0.89	0.82	0.85	0.77	1.02	1.11	0.73